Die approbierte Originalversion dieser Diplom-/Masterarbeit ist in der Hauptbibliothek der Technischen Universität Wien aufgestellt und zugänglich.
http://www.ub.tuwien.ac.at

The approved original version of this diploma or master thesis is available at the main library of the Vienna University of Technology.
http://www.ub.tuwien.ac.at/eng

DIPLOMARBEIT

Process Simulation Tool for Co-combustion of Biomass and Waste in a Circulating Fluidized Bed Combustor

ausgeführt zum Zwecke der Erlangung des akademischen Grades eines Diplom-Ingenieurin unter der Leitung von

Univ.-Prof. Dipl.-Ing. Dr.techn. Tobias Pröll

Institut für Verfahrenstechnik, Umwelttechnik und technische Biowissenschaften

eingereicht an der Technischen Universität Wien
Fakultät für Maschinenwesen und Betriebswissenschaften
von

Emanuella Rodrigues dos Santos Areal
1129474

Kleegasse 3/2.11, 8020 Graz, Österreich

geboren am 05. August 1986 in Rio de Janeiro, Brasilien

Wien, am 29.04.2016 _____

Abstract

Biomass energy promises to replace traditional fuels as a mean of sustainably energy generation. However the combustion of biofuels still struggle with low efficiencies and the release of toxic organic compounds, this scenario may change with either the development of new technology or the improvement of long-established techniques.

From all the known techniques to convert biomass into energy, the circulating fluidized bed combustion (CFBC) has proven to be a successful choice since its mass and heat transfer capabilities allows the combustion of low grade fuels with lower emissions. Also, the introduction of a new variable in the system, through the recirculation of solids, grants a better control over the heat transfer occurring inside the vessel. For that reason, the CFBC is a favourable technique for large scale energy production from biomass fuels.

On the other hand, the circulating fluidized bed combustion is a very complex process, making its design and operation challenging. To approach the inherent intricacy of this problem, a modelling of this system is proposed in this work and the software program IPSEpro was adopted, which due to its flexible programming and equation-oriented solution strategy indicates a sensible choice for the tasks this work is set to accomplish. Additionally, IPSEpro brings the possibility to reliably represent the solids flow which is a great advantage, comparing to the standard modelling of a CBFC, since it enables a more accurate representation of the recirculation flow.

The first goal of this work is to develop a model and to carry out a simulation analysis under pre determined varied conditions, based upon principles of parametric experimental design, to seek the parameters that most affect the process by using a design of experiments analysis. Furthermore, the developed model is to be validated taking as basis a valid example: the results presented by Wöß in his work, describing the pilot plant constructed in Gumpoldskirchen in a cooperation between Messer Austria GmbH and the Austrian Research Promotion Agency (FFG), and realized by Höltl during his PHD thesis. After having the model validated by a concrete example, the next step is to apply the model to a simulation of a co-firing device using a combination of biomass and waste. A range of technologies could be applied for the co-firing process, however, the use low grade fuels is the most attractive feature of this process, and in this case the CFBC may be the most suitable technology for this application.

Kurzfassung

Biomasse wird als verheißenden Ersatz für herkömmliche Kraftstoffe als Mittel zur nachhaltigen Energiegewinnung betrachtet. Obwohl die Verbrennung von Biokraftstoffen in Verbindung mit geringer Effizienz und die Freisetzung von Schadstoffen gebracht werden kann, kann dieses Szenario sich entweder mit den Entwicklungen neuer Technologien oder die Verbesserung der seit langem etablierten Techniken verändern.

Von allen bekannten Techniken, die die Biomasse in Energie konvertieren, hat die zirkulierende Wirbelschichtfeuerung sich als eine erfolgreiche Wahl aufgetaucht, da seine Masse- und Wärmeübertragungsfähigkeiten die Verbrennung von minderwertigen Brennstoffen mit geringeren Emissionen ermöglicht. Allerdings gewährt die Einführung einer neuen Variablen in dem System, durch die Rückführung von Feststoffen, eine bessere Kontrolle über die Wärmeübertragung innerhalb des Gefäßes. Aus diesem Grund ist die zirkulierende Wirbelschichtfeuerung eine günstige Technik für die Großproduktion von Energie aus Biomasse.

Auf der anderen Seite ist die zirkulierende Wirbelschichtverbrennung ein sehr komplexer Prozess, so dass das Design und der Betrieb anspruchsvoll sind. Um die inhärente Komplexität dieses Problem anzugehen, wird eine Modellierung dieses Systems vorgeschlagen, und dafür wird das Software-Programm IPSEpro angenommen, das aufgrund seiner flexiblen Programmierung und Gleichung-orientierten Lösungsstrategie, für die Aufgaben dieser Arbeit eine vernünftige Wahl zeigt. Zusätzlich bringt IPSEpro die Möglichkeit, die Feststoffströmung zuverlässig darzustellen,die ein großer Vorteil ist, da es eine genauere Darstellung der Rezirkulationsströmung ermöglicht.

Das erste Ziel dieser Arbeit ist es, ein Modell zu entwickeln und eine Simulationsanalyse unter verschiedenen vorbestimmte Bedingungen durch ein Experimentendesign Analyse durchzuführen, basierend auf parametrisch-experimentellen Design Prinzipien, um die Parameter zu suchen, die den größten Einfluss auf den Prozess einbringen. Darüber hinaus ist das entwickelte Modell mit Basis eines gültigen Beispieles validiert: die vorgestellten Ergebnisse der von Wöß in seiner Arbeit beschriebener Pilotanlage. Nachdem das Modell durch ein konkretes Beispiel validiert ist, ist der nächste Schritt, das Modell zu einer Simulation eines Mitverbrennungsausrüstung unter Verwendung einer Kombination von Biomasse und Abfall anzuwenden. Viele Technologien könnten für die Mitverbrennungsverfahren aufgebracht, jedoch ist die Verwendung minderwertigen Brennstoffen das Attraktivstes dieses Verfahrens, und in diesem Fall kann die zirkulierende Wirbelschichtfeuerung die am besten geeignete Technologie für diese Anwendung sein.

Acknowledgement

I would like to thank Prof. Tobias Pröll for the sympathy and support along this work, especially in the improvement of the quality of my work.

I am very grateful to Dipl. Ing. Stefan Bergmann for his guidance, support and kindness. I am also thankful for his patience and for the thoughtful revision, suggestions, and comments to improve the quality of this work.

I would also like to thank Dr. Erhard Perz and SimTech GmbH for the opportunity and support in the development of this work.

To my parents, I shall remain grateful my entire life for showing me that the greatest gift a child can receive is a good education.

Lastly, to my beloved husband Anderson, to whom I am deeply grateful for his patience, understanding, and love throughout the years. I appreciate sincerely all his efforts in the unfortunate task of being my first editor and reviewer and the greatest supporter of my work.

Contents

Abstract ii

Kurzfassung iii

Acknowledgement iv

Contents v

List of Figures vii

List of Tables viii

List of Abbreviations ix

List of Symbols x

1 Introduction 1
- 1.1 Motivation . . . 1
- 1.2 Outline of this Work . . . 2

2 Literature Review 4
- 2.1 Definition of Biomass . . . 4
  - 2.1.1 Properties of Biomass . . . 5
- 2.2 Conversion of Biomass to Energy . . . 10
  - 2.2.1 Thermal conversion . . . 11
  - 2.2.2 Chemical conversion . . . 15
  - 2.2.3 Biological Conversion . . . 15
- 2.3 Fundamentals of Fluidization . . . 15
  - 2.3.1 Definition . . . 15
  - 2.3.2 Characterization of particles . . . 17
  - 2.3.3 Multiparticle Systems . . . 20
  - 2.3.4 Properties of Fluidization . . . 23
- 2.4 Overview of the Circulating Fluidized Bed Process . . . 26
- 2.5 Circulating Fluidized Bed Combustor . . . 28
  - 2.5.1 State of the Art . . . 29

3 Modelling and Simulation **30**
3.1 The Software IPSEpro 30
3.2 Modelling 31
3.2.1 Model Development 31
3.3 Implementation 34
3.3.1 Formulation of the CFB Unit 34
3.3.2 Validation of the CFB Model Unit 35
3.3.3 Application of the Model Unit in the Co-combustion of biomass and waste 38

4 Results and Discussion **40**
4.1 Simple CFBC Simulation 40
4.1.1 Results 41
4.2 Simulation of the Pilot Plant 44
4.3 Simulation of the Co-combustion of Wood and Sewage Sludge 48

5 Conclusions and Outlook **52**

Bibliography **53**

List of Figures

1.1 Global energy consumption - Fuel share [1]. 2
1.2 Typical configuration of a CFB system [2]. 3

2.1 Photosyntesis process 5
2.2 Elementary composition of solid fuels [3] 6
2.3 Detail of the structure of a cell wall 8
2.4 Molecular structure of lignin, cellulose, and hemicellulose [4] 8
2.5 Ash content vs. heating value for wood and straw materials[5]. 9
2.6 Moisture influence on the heating value [5]. 10
2.7 Thermal conversion processes, its main products and uses [3]. 11
2.8 Mass loss as a function of time during combustion of wood [6]. The combustion stages can be clearly identified 12
2.9 Fluidization process 16
2.10 Fluidization bed types [7] 17
2.11 Typical size distribution of a particle set of a catalyst designed for fluidized reactors [7]. 22
2.12 Pressure Drop x Superficial Velocity Diagram. The dotted line represents the slight increase in the pressure drop due to the recirculation[8]. 24
2.13 Typical configuration of a circulating fluidized bed [2] 27

3.1 Structure of the software IPSEpro 31
3.2 Flowsheet of the circulating fluidized bed combustion process in IPSEpro 35
3.3 Flowsheet of the CFBC pilot plant in IPSEpro 37
3.4 Synergy effects between fuels in co-combustion processes [9] 38
3.5 Flowsheet of the co-combustion process 39

4.1 Effect of factors on the selected outputs per experiment 44
4.2 Operational points considered for the simulation of the pilot plant [10] 45

List of Tables

2.1 Concentrations (% dry matter) of major elements in natural solid biomass fuels in comparison to coal and lignite. 7
2.2 Operational points of some combustion systems for comparison [2]. . . 28

3.1 Elementary composition of the fuel used for the simulation of the CFBC model 36
3.2 Elementar composition of the sewage sludge used as fuel [10] 37
3.3 Operational parameters for the simulation of the co-firing process . . . 39

4.1 Input factors and output variables chosen for the simulations 41
4.2 Design of experiments 42
4.3 Results of the design of experiments simulations 43
4.4 Factors with the most effect per experiment 44
4.5 Input values applied to the operational points of the pilot plant simulation 46
4.6 Results Comparison of the Power Plant Simulation 47
4.7 Continuation: Results Comparison of the Power Plant Simulation . . 48
4.8 Thermal efficiency of the co-combustion process 49
4.9 Gas drain composition of the co-combustion of sludge and wood . . . 50
4.10 Gas drain results of the simulations of the combustions of Coal and Spruce 51

List of Abbreviations

CFB	Circulated Fluidized Bed
CFBC	Circulated Fluidized Bed Combustor
LHV	Lower Heating Value
HHV	Higher Heating Value

List of Symbols

A	Area
Ar	Archimedes number
C_D	Drag coefficient
d	Diameter
η	Efficiency
ϵ	Porosity
ϕ	Sphericity
g	Acceleration of gravity constant
H	Enthalpy
λ	Air fuel equivalent ratio
μ	Viscosity
ρ	Density
p	Pressure
P	Power
Q	Heat
Re	Reynolds constant
S	Surface area
T	Temperature
V	Volume

1 Introduction

1.1 Motivation

The current global energetic scenario drives the society towards renewable energy solutions to deal with the issues created by a fossil fuel-based energetic matrix. Problems as environmental and sustainability concerns need to be addressed by new energy technologies. Biomass emerges as a very promising renewable energy source showing potential to sensibly contribute to a future sustainable energy mix.

Biomass was the main energy source since the dawn of humanity until the Industrial Revolution when coal and oil became of more importance in order to follow the development outbreak [11][5]. Nowadays, biomass corresponds to 10% of the global annual primary energy consumption according to the World Energy Resources (WER) Survey of 2013 [12]. Though most of it comprises traditional biomass used for domestic purposes like cooking and heating in a non-sustainable manner which means low efficiencies and high release of toxic organic compounds. However, if correctly supervised, the increased utilization of bioenergy could boost the global energy supply while contributing to the reduction of CO_2 emissions. Furthermore, residue and waste can be exploited as biomass sources, reducing garbage disposal problems and providing a better use of resources. Figure 1.1 shows the current fuel share of energy consumption and a projection for 2040 as reported by the Institute for Energy Research (IER) [1] using data from the Annual Energy Outlook 2013 report by the Energy Information Administration (EIA) agency. According to this prediction, biomass contribution will closely double its share, representing a fast growth market for the next years.

There are several techniques to convert biomass into an useful energy product [11]. Combustion is currently the the most used process for obtaining bioenergy and amounts to 90% of its global production [3]. A variety of biomass combustion systems have been developed throughout the years and those range from very simple (e.g. residential stoves and boilers) to highly complex processes (e.g. CFBC). The circulating fluidized bed combustion (CFBC) has proven to be a successful choice for the burning of solid fuels such as biomass, especially due to its mass and heat transfer capabilities, which allows the combustion of low grade fuels with lower emissions. On Figure 1.2 a basic scheme of a CFBC is shown.

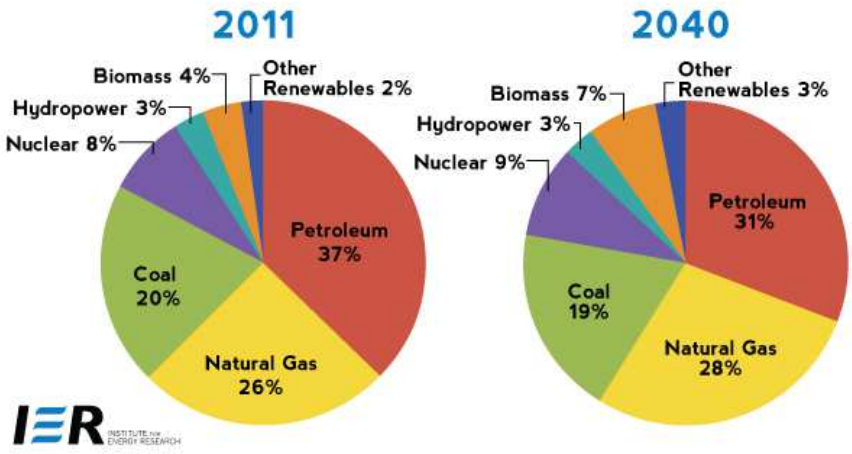

Figure 1.1: Global energy consumption - Fuel share [1].

1.2 Outline of this Work

The main goal here is to present and study the circulating fluidized bed as a viable technique for biomass combustion. The software IPSEpro is used to simulate different conditions in which the system could operate. An example flowsheet based on the Messer pilot plant is built to evaluate the behaviour of this specific CFBC system when varying some of its key parameters, for example, the bed temperature, the input O_2 concentration, and the fluid velocity.

This work is divided into five chapters, including this introduction. Chapter 2 provides a background to some of the subjects addressed along the text and gives a basis to its understanding. Chapter 3 gives a more detailed description of a CFBC and how it was modelled and in the end, Chapter 4 presents the results obtained along with a discussion of the development. Finally, Chapter 5 concludes this work giving a brief summary of its accomplishments and an outlook for future advancement.

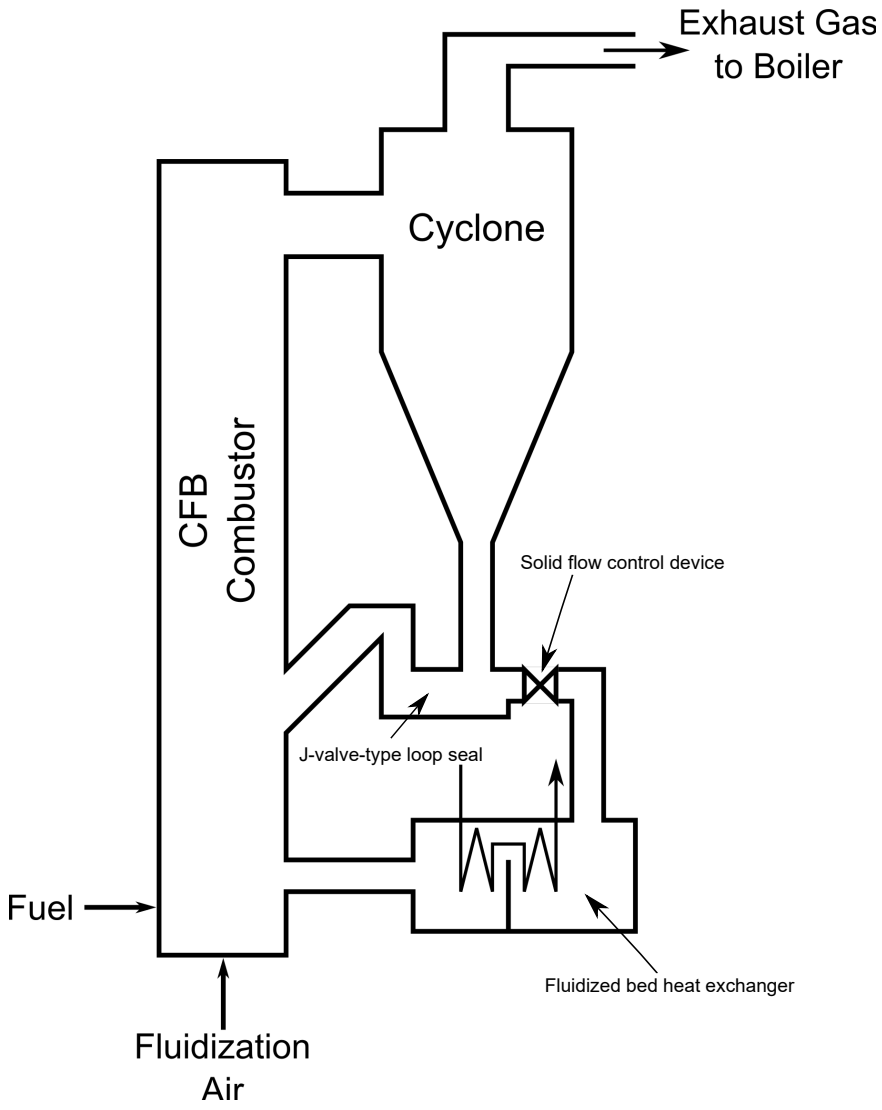

Figure 1.2: Typical configuration of a CFB system [2].

2 Literature Review

2.1 Definition of Biomass

Biomass refers to every organic material which has its origin in a living organism. It comprises living or dead (not fossilized) plant and animal matter, their residues (e.g. animal excrement), and any waste resulting from a transformation or use of the material (e.g. municipal and industrial waste)[5].

Biomass is an energy carrier and differs from other organic energy carries, like petroleum, for its fast matter renovation and, therefore, it is called a renewable energy source [11]. The energy in the biomass is stored in the form of carbohydrates essentially consiting of $C_6H_{12}O_6$ units carbon and is obtained by plants through photosynthesis, as simply depicted in Figure 2.1. During this process, the sunlight energy is converted into chemical energy which can be released later according to the vegetal needs, providing energy for the plant's physiological activities. Plants can be subsequently eaten by animals and converted into animal biomass, but this work will focus exclusively on the herbal biomass. The overall chemical reaction of photosynthesis can be written in a simplified manner as

$$Sunlight + CO_2 + H_2O + Nutrients \rightarrow C_nH_{2n}O_n + O_2 \ , \tag{2.1}$$

where $C_nH_{2n}O_n$ represents the organic matter and the nutrients are a mixture of nitrates (NO_3), phosphates (PO_4), iron (Fe), among others, according to the plants needs.

Common biomass examples used as energetic sources are wood, agricultural (such as sugarcane bagasse), forestry, industrial (such as paper or lumber mill residue), and urban waste. The relevant sources for this work will be described in the following.

Wood and Agricultural Residues

Woody biomass is the most commonly used biomass as an energy source. It comprises forestry products, wood chips, sawdust, bark, and several other wood by-products. Agricultural products that could be used for the energetic production are its residues or the byproducts of its processing. Agricultural residues include parts of the crops which are not supposed to be used for its primary goal, such as food, feed or fibre. Some

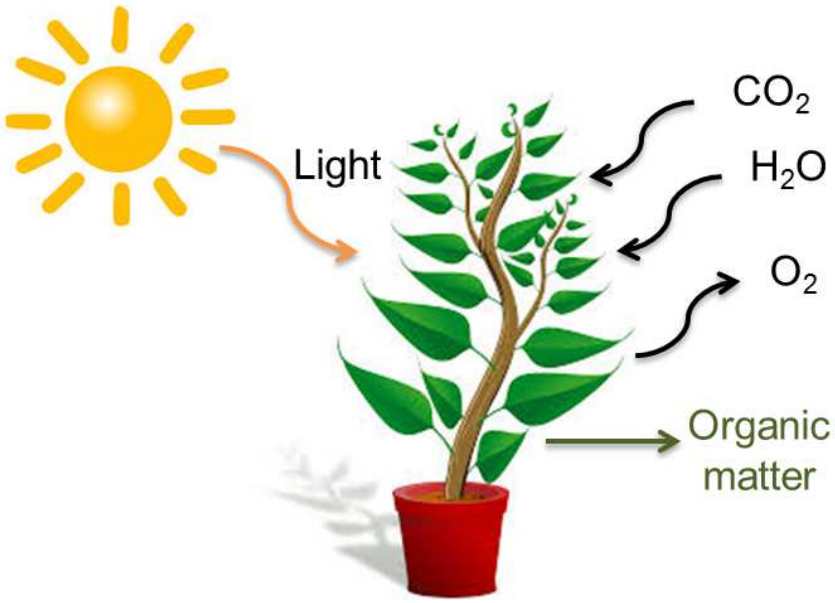

Figure 2.1: Photosyntesis process

examples of residues are straw, sugarcane bagasse, rice husk, nut shells and fruit pits. Energy crops are also a sustainable alternative to produce energy from biomass. They are low-cost and low-maintenance plants which are grown specially with the purpose of producing energy. Energy crops can be grasses, like the switchgrass, or some fast growing trees like poplar and willow for cold climates, sweetgum and cottonwood for warmer climates [13].

Solid Waste

Solid waste biomass includes those originated from municipal and industrial residues. Home waste residues include paper, containers (plastic and metal), aluminium cans, and food leftovers, as well as sewage. For industrial and commerce waste, it consists mostly of paper, wood, and metal scraps, as well as agricultural waste products. Since its composition varies widely, it is difficult to have a defined standard. However, there are a large number of online databases [14][15][16] that can be used as reference to obtain an approximation in some cases.

2.1.1 Properties of Biomass

The inherent properties of a fuel source determine the available technology that could be employed to efficiently generate energy. Furthermore, a careful investigation of the fuel properties brings a better understanding on the complications that may arise

during the fuel processing. Described bellow are some of the properties that are of concern in this work.

Elementary Composition

The most important characteristic of a woody type of fuel is the elementary composition distribution of carbon (C), hydrogen (H), and oxygen (O), although other elements also appear in the molecule in different concentrations depending on the type of wood [5][17]. The elementary composition may act on different properties of the compound. For instance, the calorific and heating values, and the air demand are all affected by the amount of carbon, hydrogen, and oxygen on the fuel molecule. The amount of carbon also affects the particle emission which is relevant for environmental impacts during the burning of biomass. Other elements on the molecule may also have an impact on the emissions rate and the most commonly present are nitrogen(N), which increases NO_x and N_2O emissions, sulphur (S), that contributes to the SO_x emissions as well as particle emissions [5]. Magnesium (Mg), potassium (K), calcium (Ca), and some heavy metals can contribute to the modification of the properties of the ash produced. A more detailed description can be found in the book from Kaltschimitt et al [5]. Figure 2.2 shows the chemical distribution of the main elements on some solid fuels and its influence on the heating value and on Table 2.1 the elementary composition of some fuel/biomass types are displayed [5].

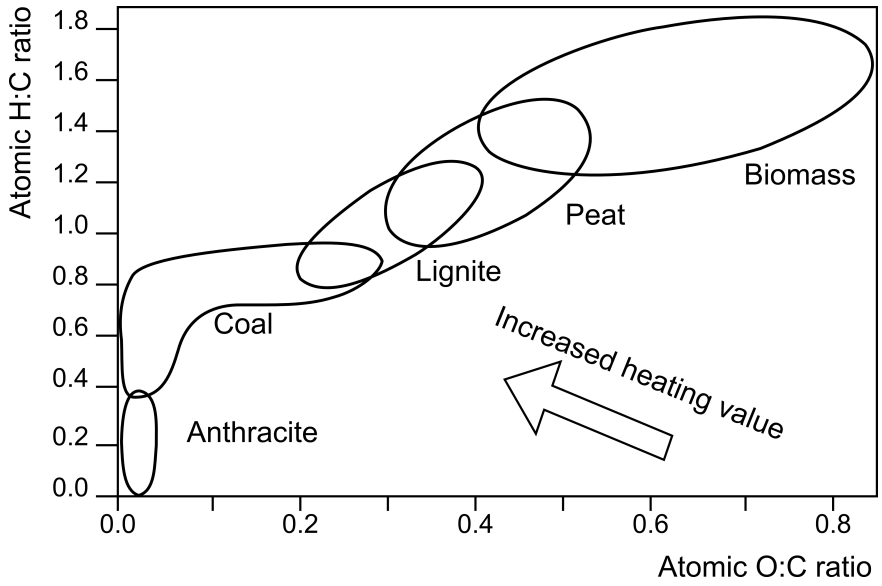

Figure 2.2: Elementary composition of solid fuels [3]

Fuel or Type of Biomass	C	H	O	N	K	Ca	Mg	P	S	Cl
Coal	72.5	5.6	11.1	1.3					0.94	< 0.13
Lignite	65.9	4.9	23.0	0.70					0.39	< 0.1
Spruce wood (w/ bark)	49.8	6.3	43.2	0.13	0.13	0.70	0.08	0.03	0.015	0.005
Poplar (short rotation)	47.5	6.2	44.1	0.42	0.35	0.51	0.05	0.10	0.031	0.004
Bark (coniferous)	51.4	5.7	38.7	0.48	0.24	1.27	0.14	0.05	0.085	0.019
Corn husk	45.7	5.3	41.7	0.65					0.12	0.35
Wheat straw	45.6	5.8	42.4	0.48	1.01	0.31	0.10	0.10	0.082	0.19
Wheat whole	45.2	6.4	42.9	1.41	0.71	0.21	0.12	0.24	0.12	0.09
Wheat grain	43.6	6.5	44.9	2.28	0.46	0.05	0.13	0.39	0.12	0.04

Table 2.1: Concentrations (% dry matter) of major elements in natural solid biomass fuels in comparison to coal and lignite.

Molecular Composition

A solid biomass typically contains cellulose, lignin, and hemicellulose molecules which altogether represent more than 95% of the dry mass of a plant [5]. These molecules are present in the plants' cell wall and act in its structure and stability. Cellulose consists of a polymeric chain of glucose and it is the framework of the cell wall, granting tensile strength to the vegetable. Lignin does not exist alone in the plant matter, it is always accompanying the cellulose, and confers pressure stability through its cementing and stiffening effect. Hemicellulose is an amorphous molecule, consisting of a matrix of polysaccharides which is composed of different monomeric units of pentoses, hexoses and uronic acids. The hemicellulose has a variety of functions ranging from flexibility and support of the cell wall to supply material. The distribution of these molecules directly affects the behaviour of the biomass as a fuel. The relative proportion of cellulose and lignin on the vegetable, for instance, is a determining factor in deciding whether or not a plant is suitable as an energy crop [17]. This distribution is directly linked to the total carbon content which is essential to determine the calorific value of a plant's dry matter, hence, impacting on the energy contained in it. Along these lines, an increase of the lignin or of the extractives content leads to a higher carbon content and, consequently, to an increase of the calorific value. On Figure 2.3 an example of the structure of the cell wall and how these molecules are there allotted is depicted and on Figure 2.4 the molecular structures of lignin, cellulose, and hemicellulose are illustrated.

Calorific Value

The calorific value, also called heating value, constitutes the amount of energy present in the fuel, and there are actually multiple values depending on how this energy is measured. The fuel yields different caloric values depending on whether the pressure

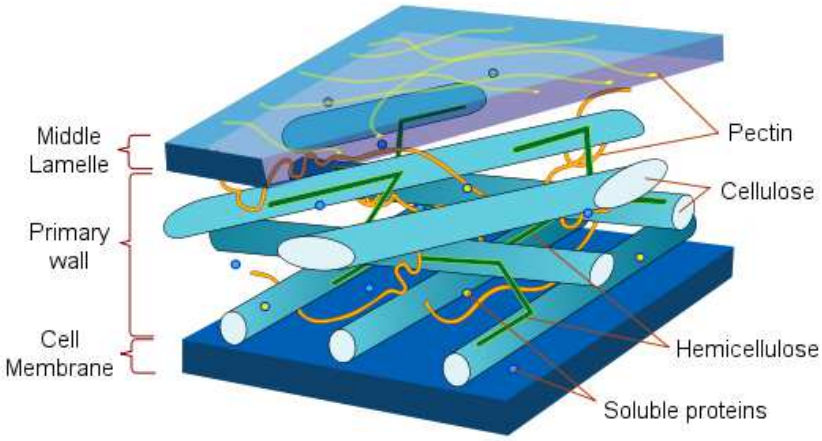

Figure 2.3: Detail of the structure of a cell wall

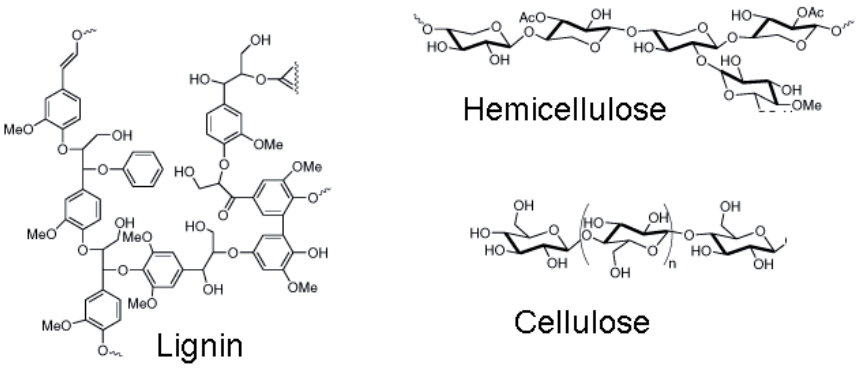

Figure 2.4: Molecular structure of lignin, cellulose, and hemicellulose [4]

or volume is made constant during measurements, or by considering product water in either condensed or vapour phase, or still by measuring the internal energy or the enthalpy of combustion [18].

The net calorific value, for instance, is defined as the energy released when the fuel is completely oxidized without considering the heat of vaporization of water. This may also be called the lower heating value (LHV). The gross calorific value, on the other hand, takes into consideration the heat of vaporization meaning that the measured value will be higher and that it can also be called as the higher heating value (HHV).

Ash Content

Ash is defined as the inorganic residues of the combustion of biogenic materials. The ash-forming compounds are present in the biomass in the form of salts which are either bound to the carbon structure or are mineral particles resulting from transport or harvesting. The ash content can influence two important aspects of the combustion. It can lower the heating value of the fuel and increase the environmental damage by increasing the particles emission and deteriorating the quality of the residues. Figure 2.5 shows the relationship between the ash content and the calorific value.

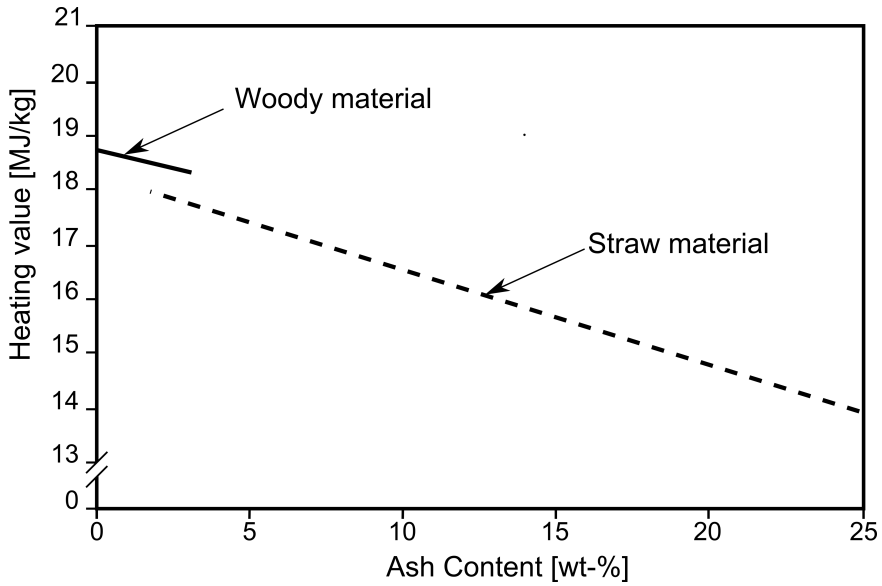

Figure 2.5: Ash content vs. heating value for wood and straw materials[5].

Moisture

Moisture is the relative amount of water contained in the fuel. It directly affects the heating value, hindering the combustion reaction as increased. The limit moisture content for the majority of biomass fuels is around 65% on a wet basis (mass of water per mass of moist fuel) [18]. When the moisture exceeds this limit the energy released by the combustion is not enough to provide heat to sustain the reaction and to evaporate the water contained in the fuel, and an additional fuel, like natural gas, may be required. As it will be debated in Section 2.2.1, moisture is one of the most relevant properties of a fuel, because it can ultimately define if a combustion process can be sustained or not. The moisture content may also have an effect on the storage feasibility and fuel weight of the biomass, and the combustion temperature. Figure 2.6 below shows a correlation between the calorific value and the water content.

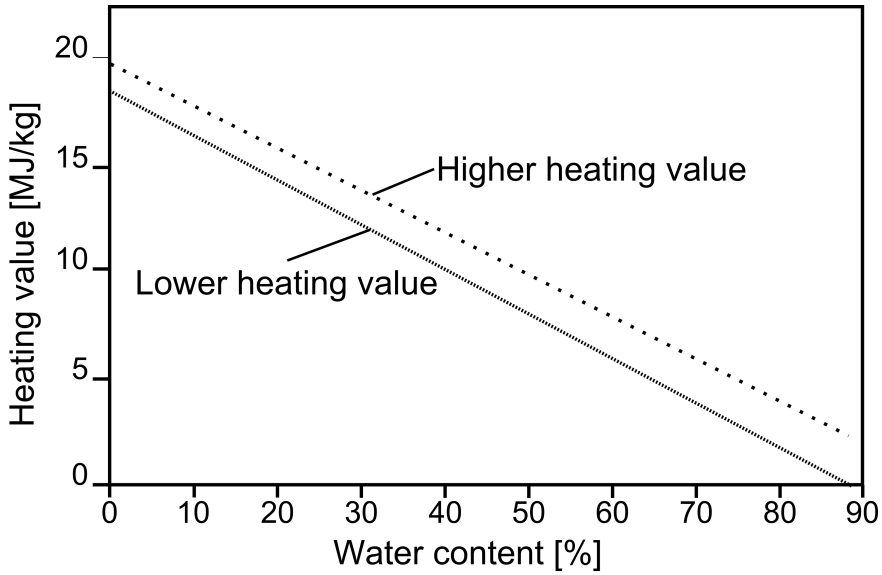

Figure 2.6: Moisture influence on the heating value [5].

Physical and Mechanical Properties

Properties as shape and particle size distribution defines the technical aspects of the employed apparatus, like the type of furnace used or mechanical systems needed. Moreover, particle geometry affects directly the ignition ability of the fuel and, consequently, its risk of explosion, which concerns safety. Other characteristics, like the bulk and particle densities, as well as the bridging tendency, affect mainly its storage and transport ability. A more detailed description of the effects of each property of biomass can be found in the literature [5][17].

2.2 Conversion of Biomass to Energy

There are a variety of options available to utilize the energy from biomass sources. Conversion technologies can either directly release the energy in the form of heat or electricity, or convert the biomass into another energy carrier form, liquid biofuel or combustible biogas, for instance. These technologies are in different stages of development, where combustion is the most advanced one and also most frequently used. The choice of an appropriate technology depends on a wide range of factors, for example, the type of biomass available and the purpose of the resulting products. An overview of the available technologies for biomass conversion, their main products, and their potential end uses are shown in Figure 2.7. In general, the conversion process can be divided into three categories: thermal, chemical, and biological conversion. A

particular focus on thermal conversion will be laid in the following discussion, since it comprises the main topic of this work.

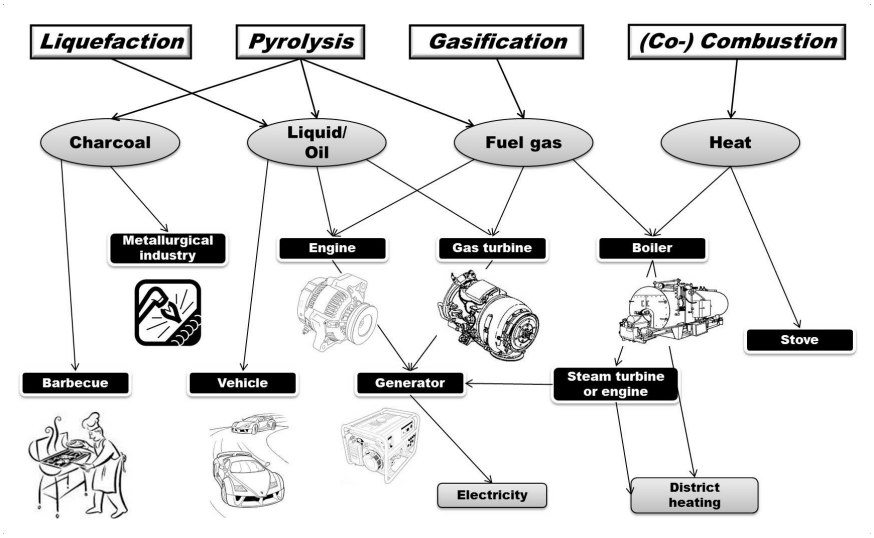

Figure 2.7: Thermal conversion processes, its main products and uses [3].

2.2.1 Thermal conversion

In thermal conversions, heat is used to release the stored energy in the biomass. The major methods for thermal conversion of biomass for energy purposes are combustion, gasification, and pyrolysis. The primary products of these processes may be in the form of energy carriers such as charcoal, oil, and gas, or in the form of heat. These are described in detail bellow.

Combustion

Biomass combustion is a complex process and involves a wide variety of physical and chemical factors. The characteristics of this process is very dependent on the properties of the fuel and on its field of application. For instance, for small-scale units a batch mode with a natural air draught may be well-suited. However, medium to large-scale units operate continuously only with a forced draught.

Combustion can ideally be defined as a complete oxidation of the fuel. The resulting hot gases can be used differently, depending on the scale of the units. For small-scale units, direct heating and water heating is a common application. For large-scale, the gases can be also used to heat water in a boiler for electricity generation.

The combustion process consists of a series of consecutive heterogeneous and homogeneous reactions and can be divided into five general process steps: drying, devolatization, gasification, char combustion, and gas-phase oxidation. The relative importance of these steps will vary according to the technology implemented, the fuel properties, and the process conditions. The first step in the combustion process is always drying followed by the pyrolysis/gasification of the fuel, and finally, char oxidation. For the batch combustion of a small particle, these stages can be distinguishably separated, as seen in Figure 2.8. Although, in larger particles, these stages may overlap. For continuous combustion processes, these stages occur in various sections of the reactor. Hence, the optimization for zones of different process steps is possible, which can be of great advantage, especially regarding the control of pollutants production.

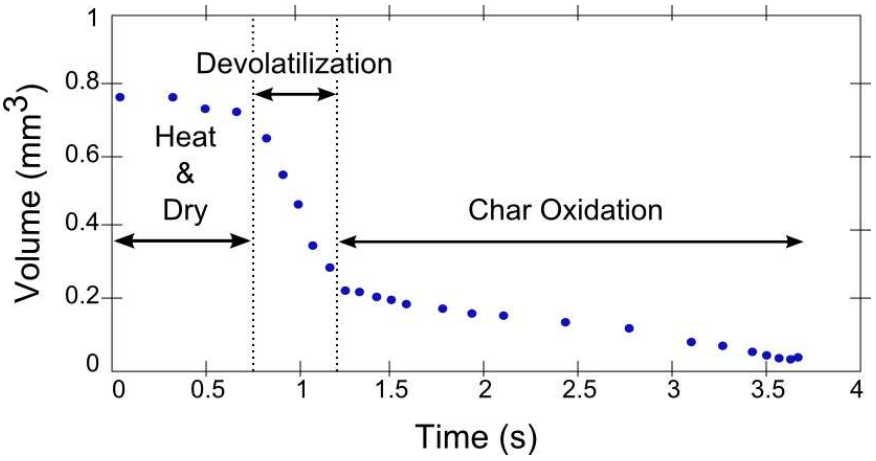

Figure 2.8: Mass loss as a function of time during combustion of wood [6]. The combustion stages can be clearly identified

After entering the combustor environment, the fuel is heated up and any moisture contained in it will evaporate. This lowers the chamber temperature and, consequently, slows the process down, since part of the energy released by the overall process is used for the vaporization. Thus, there is a maximum moisture concentration for each material that should not be overstepped, otherwise the temperature will get too low and the combustion process cannot be maintained. For that reason, the moisture content in the fuel is a critical variable for the combustion process.

With further increase in temperature devolatilization begins by thermally cracking the weak bonds in the structure. The release rate of volatiles increases and ignition of the volatile matter may occur, if the conditions are favourable. This creates a layer on the surface of the fuel preventing oxygen from reaching it. Thus, the devolatilization on the surface occurs in the absence of an oxidizing agent, called pyrolysis. The temperature continues to increase and heads towards its maximum. The loss of volatile matter reduces the release rates and the extinction of the volatiles flame is very likely. The oxygen can then reach the fuel surface and the char oxidation occurs.

The fuel oxidation can be generally expressed by

$$C_mH_n + (m + n/4)O_2 \rightarrow mCO_2 + (n/2)H_2O + Heat \ , \tag{2.2}$$

where C_mH_n represents a hydrocarbon fuel which is mostly the case in combustion. For the burning of hydrocarbons the products of a complete combustion are CO_2, water and heat, being it an exothermic reaction. For different fuel types and/or for incomplete combustion these products vary. For instance, biomass fuels have sulphur in their composition which leads to the formation of SO_2 as a product of its complete combustion. This is a very simple representation of a combustion reaction for, in reality, several reversible elementary reactions occur simultaneously which is a very onerous task to describe, even for a simple fuel such as methane.

Variations in some parameters may negatively affect the reaction rate of the combustion process, causing an incomplete reaction. For example, lack of oxygen due to either insufficient supply or to inadequate mixing of air and fuel, creating fuel-rich zones. A residence time in the reactor that is too short also leads to the incompletion of the combustion, as well as low temperatures. The reaction rate of a combustion reaction can be formulated as

$$\begin{aligned} & a \cdot Fuel \ + \ b \cdot Oxidant \ \rightarrow \ c \cdot Product \\ & \frac{d[Product]}{dt} = k \cdot [Fuel]^a \cdot [Oxidant]^b \qquad \left[\frac{mols}{m^3 s}\right] \ , \end{aligned} \tag{2.3}$$

where k is the reaction rate constant and can be expressed by

$$k = \alpha \cdot T^{\beta} \cdot exp\left(\frac{E}{R \cdot T}\right) \ , \tag{2.4}$$

where α, β, E, and R are the pre-exponential factor, the temperature exponent, the activation energy, and the universal constant of gases, respectively. The influence of mixing can be expressed in the concentrations of fuel and oxidant and its respective coefficients, while the impact of temperature is indicated in the constant k, where it has an exponential effect.

The fundamental parameter in the combustion process is the air-fuel equivalence ratio (λ) which is defined as [5]

$$\lambda = \frac{w_{O_2}}{w_{O_2}^{st}} \tag{2.5}$$

where w is the weight fraction and the index st means at stoichiometric conditions. This parameter is used to assure that enough oxygen is being supplied for a complete

reaction to happen. For $\lambda > 1$ the mixture is called lean and there is an excess of air (oxygen) in the mixture, for $\lambda = 1$ the supplied amount of fuel and oxygen matches that in stoichiometric conditions, and for $\lambda < 1$, the mixture is called rich and there is a surplus of fuel in the mixture. For combustion processes a $\lambda \geqslant 1$ is required.

As a result of an incomplete combustion, there are a variety of pollutants that can be formed [6]. The concentration of each component depends on the kind of fuel used. They can be categorized as:

1. incomplete combustion products such as CO, C_nH_m, tar, unburned carbon, H_2, HCN, NH_3, and N_2O;
2. complete combustion products such as NO_x, CO_2, and H_2O;
3. ash and solid particles contaminants.

Gasification

Similarly to combustion, gasification is another conversion process employed to biomass, which is then converted to a secondary energy carrier (heat, electricity, or other fuels). Gasification process is analogous to the combustion: a thermal degradation process in the presence of an oxidant, which can be either air, oxygen, steam or CO_2, only it is optimized to a maximum gas yield. The product gas , also called synthesis gas, is composed mostly of a mixture of carbon monoxide (CO) and hydrogen (H_2) and it can be used as reagent in a synthesis process (Fischer-Tropsch process or Methanol synthesis, for instance) to yield a higher quality product. Alternatively, the product gas can be burned in a boiler for the production of hot water and steam, or even in a gas turbine for the production of electricity.

Pyrolysis

When the thermal degradation takes place in the absence of an oxidizing agent, it is called pyrolysis and it produces mainly tar, charcoal, and some lower molecular weight gases. In some oxygen-rich fuels, which is the case for biomass, CO and CO_2 can also be formed. The products formed can be used in a variety of applications. Char can be improved into activated carbon, which can be used in the metallurgic industry, as well as a domestic cooking fuel. Methanol and liquid hydrocarbons can be synthesized from the pyrolysis gas, which can also be used for heat and power generation. In addition, the tar, also called pyrolysis oil, can be converted into a high-grade hydrocarbon liquid fuel and also used for heat and electricity production [3].

2.2.2 Chemical conversion

There are assorted chemical conversion processes that can be used on the conversion of biomass into more useful energy carriers. Some of the most commonly used processes are the Fischer-Tropsch conversion and the Methanation. The Fischer-Tropsch process converts a mixture of hydrogen (H_2) and carbon monoxide (CO), which are the usual products of the gasification of biomass, into liquid fuels (e.g. ethene, propene, LPG, naphta, diesel, and gasoline). Similarly, the methanation process uses a mixture of hydrogen (H_2) and carbon monoxide (CO) in the proportion of 3:1 to obtain methane (CH_4) and water (H_2O) as products [19][20].

2.2.3 Biological Conversion

Since biomass is a natural material, there are a variety of highly efficient biochemical processes in nature to break down the molecules in the biomass by using the enzymes of some micro-organisms. Some common examples of this conversion processes frequently used in the industry are anaerobic digestion, fermentation, and composting [21][22][23].

2.3 Fundamentals of Fluidization

2.3.1 Definition

Fluidization is an operation where solid particles are suspended in a gas or liquid, forming a state that resembles a fluid. The fluidized state presents peculiar characteristics that are rather appealing for engineering purposes, e.g. rapid mixing and excellent temperature control. In this section basic principles for the comprehension of this phenomenon will be presented.

The particle bed assumes different behaviours according to the velocity of the fluid passing up through it. If the velocity is low, the fluid percolates through the empty spaces between the particles which stay stationary. This state is called a fixed bed. As the fluid velocity increases, the particles start to distance from each other and some vibration and movement in some areas are observed. This is known as expanded bed. This situation persists until such a velocity is reached where all the particles are suspended by the up flow of the fluid. At this point the fluid drag force is balanced by the weight of the particles. The bed is considered fluidized and this is the point of minimum fluidization. From this point, as the fluid velocity increases, the pressure drop along the bed stays approximately constant and the bed expands. Figure 2.9 depicts this procedure.

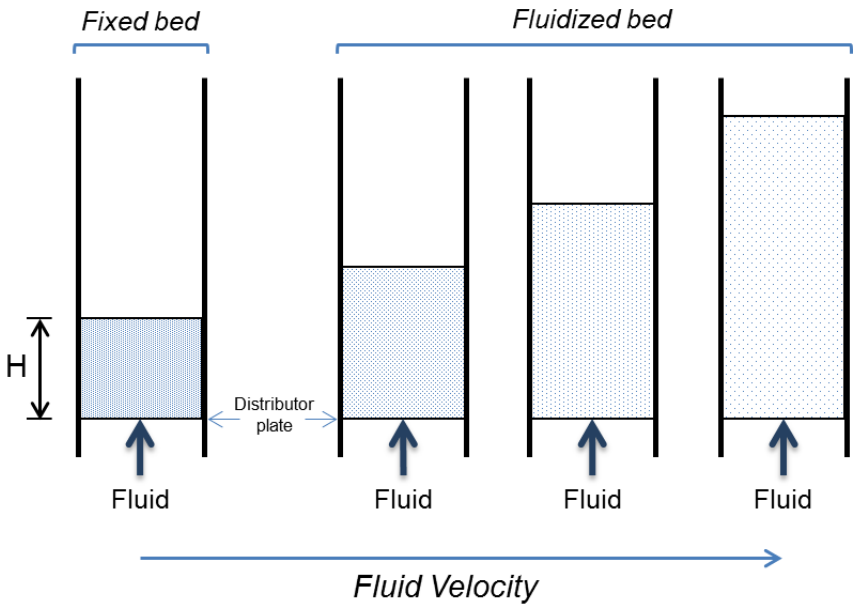

Figure 2.9: Fluidization process

Above the minimum fluidization point, the bed shows different behaviours according to the fluid physical properties. In liquid-solid systems it usually results in a uniform gradual expansion of the bed. Any major flow instabilities are damped and the bed has a visual homogeneity. With gas-solid systems such a well-behaved appearance is achieved only under special conditions of fine light particles with dense gas. Under normal conditions, some large instabilities are observed, such as bubbling and channelling of gas. At a high flow rate the stream becomes more turbulent and the solids agitate vigorously. The gas bubbles coalesce and grow as they go through the bed and, if the bed has a high height-to-diameter ratio, the bubble can grow to occupy the whole dimension across the diameter of the container [7].

For sufficiently high flow rates, the gas velocity exceeds the terminal velocity and the particles become entrained. The bed assumes then a turbulent behaviour and any increase in velocity pushes the particles out with the fluid. For a steady state operation, these particles have to be collected by a cyclone and returned to the bed. Figure 2.10 depicts the different types of beds described above.

Fluidized beds are largely used in industrial processes, especially due to their high degree of mixing, and the high heat and mass transfer coefficients between the solids and the fluid. An additional advantage is the constant and homogeneous temperature of the bed, which creates a suitable environment for the processing of heat sensitive materials [24]. There are innumerable applications such as in the catalytic conversion of hydrocarbons, drying, combustion, and coating.

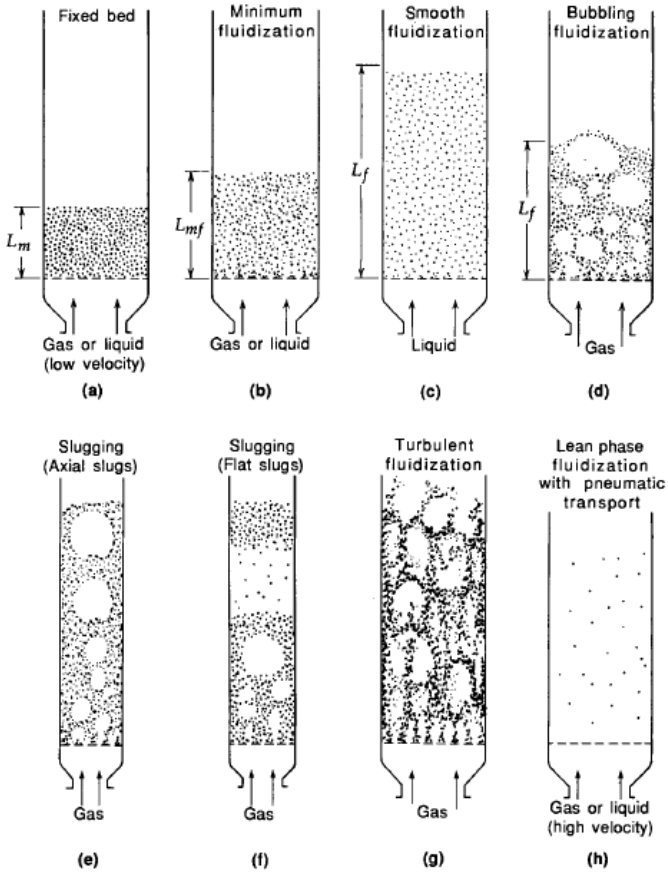

Figure 2.10: Fluidization bed types [7]

2.3.2 Characterization of particles

The complete characterization of a single particle includes the measurement and definition of size, density, shape, and surface morphology [25]. Particles might present irregular shape and different surface morphology, therefore, there are assorted approaches – depending on the application – to characterize particles.

Size

Particle size is defined as one or more of the particle dimensions (e.g. height, width, radius), in such a way that, the particle become fully described in the space. For instance, for spherical shapes the diameter is the characteristic dimension. Regular particle shapes are easily characterized by two or three of its dimensions. However, particles of practical interest don't often have a regular shape and the definition of a characteristic dimension become somewhat complicated. Hence, different measures

have been defined to characterize irregular particles and the most common are summarized bellow [25].

Volume diameter

The volume diameter, d_v, is defined as the diameter of a sphere having the same volume as the particle and can be expressed mathematically as

$$d_v = \left(\frac{6V_P}{\pi}\right)^{1/3} , \tag{2.6}$$

where V_P is the volume of the particle.

Surface diameter

The surface diameter, d_s, is defined as the diameter of a sphere that has the same surface area as the particle, and can be written as

$$d_s = \left(\frac{S_P}{\pi}\right)^{1/2} , \tag{2.7}$$

where S_P is the surface area of the particle.

Surface-volume diameter

The surface-volume diameter, d_{SV}, is defined as the diameter of a sphere with the same surface area-to-volume ratio as the particle. This is also known as the Sauter diameter and can be written as

$$\begin{aligned} d_{SV} &= \frac{6V_P}{S_P} \\ &= \frac{{d_v}^3}{{d_s}^2} . \end{aligned} \tag{2.8}$$

$$d_{SV} = \frac{6V_P}{S_P} = \frac{{d_v}^3}{{d_s}^2} . \tag{2.9}$$

Sieve diameter

The sieve diameter, d_A, is defined as the width of the minimum square aperture in the sieve screen through which the particle passes.

Stokes diameter

The Stokes diameter, d_{st}, is the free-falling diameter of the particles in the Stokes law region and can be calculated from

$$d_{st} = \sqrt{\frac{18\mu U_t}{(\rho_P - \rho_f)g}} \ , \tag{2.10}$$

where U_t is the terminal velocity of the particle.

Shape

Particles can appear in an infinite amount of shapes and most of the particles of interest are irregular in shape. Thus, empirical factors were proposed to describe non-spherical shapes of particles. The most commonly used factor, called sphericity, ϕ, is defined as

$$\phi = \frac{Surface\ area\ of\ volume-equivalent\ sphere}{Surface\ area\ of\ particle} = \left(\frac{d_v}{d_s}\right)^2 = \frac{d_{SV}}{d_v} \ . \tag{2.11}$$

The sphericity can assume values from 0 to 1 and, for a true sphere, $\phi = 1$.

Density

Particles may present any convex (e.g. spherical) or concave shape (e.g. torus), hence density measures must account for shape particularities, in order to avoid significant deviations from the reality [25]. The definition of density for non-porous particles is simply defined by

$$\rho = \frac{M_P}{V_P} \ , \tag{2.12}$$

where M_P and V_P are the mass of the particle and the total volume of the particle (including the pores, if there are any), respectively. Considering the pores inside a particle the density would be

$$\rho_P = \frac{M_P}{V_P - V_{Pores}} \ , \tag{2.13}$$

where V_{Pores} is the volume of the pores. Some techniques for particle characterization can be found in literature [25].

2.3.3 Multiparticle Systems

Fluidization processes require a large amount of particles which presents a wide spread size distribution, due to the difficulties to produce or to find a set of particles with homogeneous size. Therefore, the particle aggregate must be properly described to include the influence of different size distributions to the bed. There are a fairly amount of models to describe multi-particle systems [25] and each application may demand the use of a different one. Some models are listed bellow, but many others can be found in the literature [25].

Average Particle Diameter

A set of particles may be characterized by its average particle diameter. The average size is defined depending on the particle diameter distribution. A typical average employed in fluidization processes is the harmonic mean diameter, which can be derived from the surface-volume diameter definition.

Consider N_1 esferic particles with a diameter d_1, N_2 particles a diameter d_2, and so on, according to the definition 2.9, results

$$\bar{d}_p = 6 \cdot \frac{N_1 \cdot \frac{d_1^3 \cdot \pi}{6} + N_2 \cdot \frac{d_2^3 \cdot \pi}{6} + \dots}{N_1 \cdot d_1^2 \cdot \pi + N_2 \cdot d_2^2 \cdot \pi + \dots} \tag{2.14}$$

Multiplying 2.14 by $\rho_p \cdot g$ and rearranging

$$\bar{d}_p = \frac{N_1 \cdot \frac{d_1^3 \cdot \pi}{6} \cdot \rho_p \cdot g + N_2 \cdot \frac{d_2^3 \cdot \pi}{6} \cdot \rho_p \cdot g + \dots}{N_1 \cdot \frac{d_1^3 \cdot \pi}{6} \cdot \rho_p \cdot g \cdot \frac{1}{d_1} + N_2 \cdot \frac{d_2^3 \cdot \pi}{6} \cdot \rho_p \cdot g \cdot \frac{1}{d_2} + \dots} \ . \tag{2.15}$$

Assuming that for a particle n

$$G_n = N_n \cdot \frac{d_n^3 \cdot \pi}{6} \ , \tag{2.16}$$

2.15 results in

$$\bar{d}_p = \frac{G_1 + G_2 + \dots}{G_1 \cdot \frac{1}{d_1} + G_2 \cdot \frac{1}{d_2} + \dots} \ . \tag{2.17}$$

Multiplying 2.17 by G_{total}

$$\bar{d}_p = \frac{x_1 + x_2 + \dots}{x_1 \cdot \frac{1}{d_{p1}} + x_2 \cdot \frac{1}{d_{p2}} + \dots} \ , \tag{2.18}$$

where

$$G_{total} = \sum G_n \ , \tag{2.19}$$

$$x_n = \frac{G_n}{G_{total}} \ and \tag{2.20}$$

$$\sum x_n = 1 \ , \tag{2.21}$$

$$\tag{2.22}$$

resulting in the equation for the harmonic mean particle diameter

$$\bar{d_p} = \frac{1}{\sum \frac{x_n}{d_{pn}}} \ , \tag{2.23}$$

valid only for relative standard deviation(σ/d_p) values less than 0.5.

Descriptions of aggregates solely by the mean value might result in rough approximations of the particle size effects. Especially, if the particles size presents a high standard deviation or the distribution is not-symmetrical. However, the model presented here is simple and easy to implement, and can be used to describe a large variety of particle dust used in technical applications.

Statistical Characterization

Since the characterization of the batch of solids to be used involves a distribution, it is only natural to use statistical tools to properly interpret it. For that, consider the functions p and P, which will be used to describe the size distribution of such particles, defined as

$$p_i = \left(\frac{dP}{dD}\right)_i \ ,$$
$$P = \int_0^{D_i} p \ dD \ , \tag{2.24}$$

where D_i and P are the particle size and the volume fraction of the particles smaller than D, respectively, and $p \ dD$ is the volume fraction of sizes between dD and $D+dD$. Figure 2.11 depicts the graphical form of theses functions.

Statistical treatment enables a more detailed description of the particle aggregates, thus, minimizing any problems that might arise from the deviations on the average particle size in a distribution.

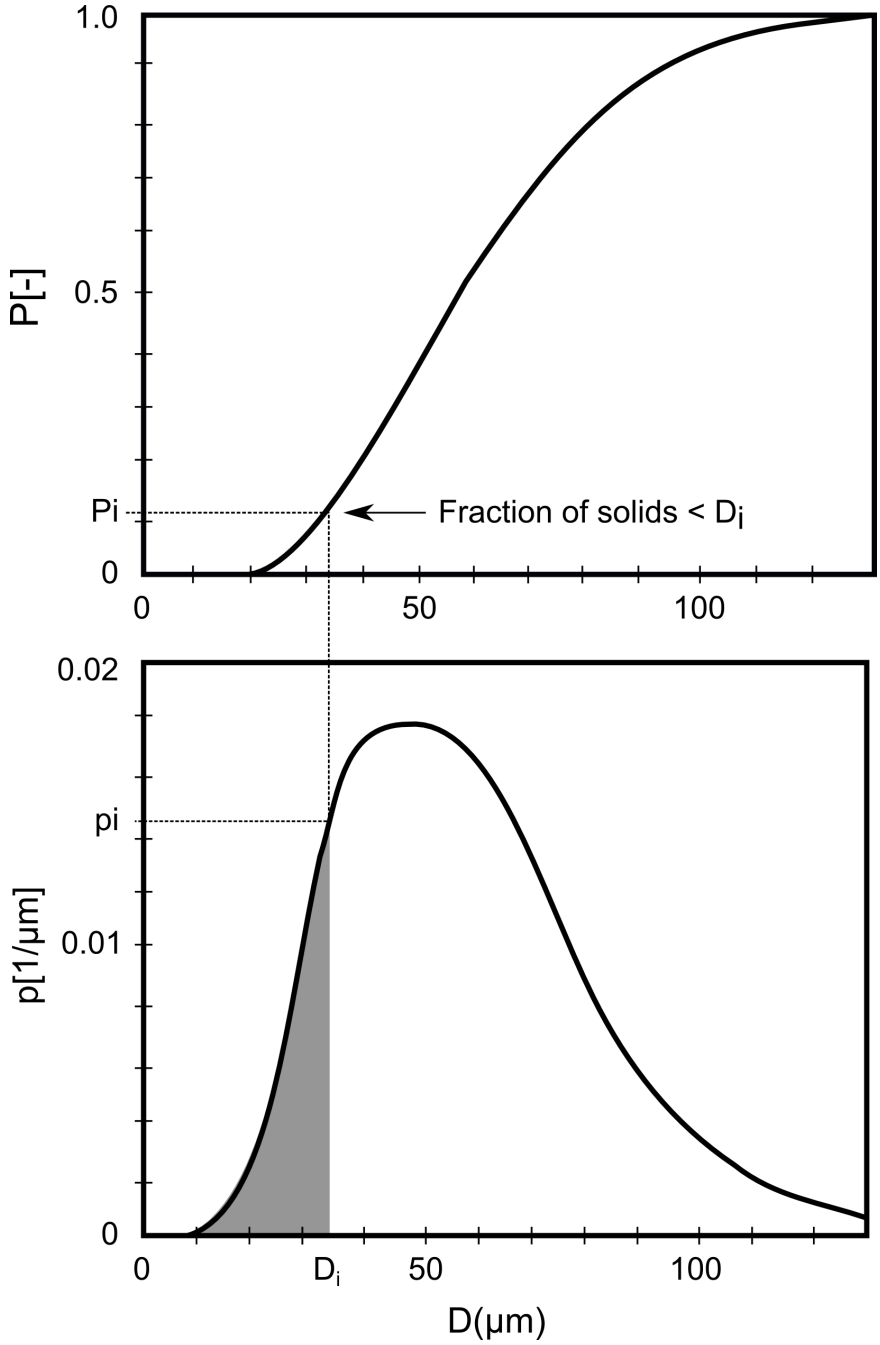

Figure 2.11: Typical size distribution of a particle set of a catalyst designed for fluidized reactors [7].

Porosity and Bulk Density

The definition of the porosity is necessary to completely characterize a bed of particles. Porosity is defined as

$$\epsilon = \frac{Total\ volume\ of\ the\ bed - Volume\ of\ the\ particles}{Total\ volume\ of\ the\ bed} \tag{2.25}$$

$$= 1 - \frac{M}{\rho_P V_b}\ , \tag{2.26}$$

where M is the total mass of the particles and V_b is the volume of the bed. Another important definition is the bulk density which can be described by

$$\rho_B = \frac{M}{V_b}\ . \tag{2.27}$$

Using (2.27), (2.25) can be rewritten as

$$\epsilon = 1 - \frac{\rho_B}{\rho_P}\ . \tag{2.28}$$

2.3.4 Properties of Fluidization

The process of fluidization can be divided into three stages according to the pressure drop and the superficial velocity. First, the bed takes the form of a fixed bed and due to its relatively low flow rate the pressure drop increases approximately proportional to the gas velocity, until it reaches the point of minimum fluidization. Thereupon, the bed starts to expand with the increase in velocity and the pressure drop stays constant up to the pneumatic transport region, where the particles become entrained and the bed is then emptied. If the particles are recirculated into the bed again, the pressure drop will slightly increase. A summary of this process is depicted in Figure 2.12 [7][8].

Pressure Drop x Superficial Velocity Diagram

The relation between pressure drop and superficial velocity can be used to better define the region where the fluidization occurs and can be particularly useful as a rough indication of the quality of the fluidization. Figure 2.12 sketches a simplified version of this relation.

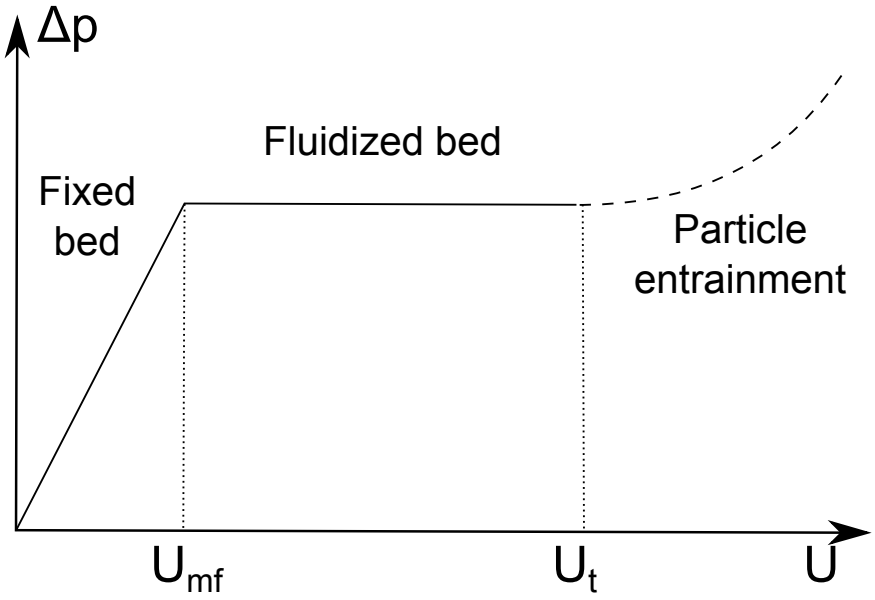

Figure 2.12: Pressure Drop x Superficial Velocity Diagram. The dotted line represents the slight increase in the pressure drop due to the recirculation[8].

Pressure Drop in a Fluidized Bed

A particle bed will change from fixed bed into a fluidized bed if the resistance force to the gas flow is equal to the total weight of the particles forming the bed; taking account of the buoyancy and the proportion of particles present, the pressure drop can be described in a fluidized bed as

$$\begin{aligned} \Delta p A_t &= A_t H_b (1-\epsilon) \left[(\rho_p - \rho_g) g \right] \ , \\ \frac{\Delta p}{H} &= (1-\epsilon)(\rho_p - \rho_g) g \ . \end{aligned} \tag{2.29}$$

where Δp is the pressure drop across the bed, A_t is the cross-sectional area of the tube where the bed is contained, H is the height of the bed, and g is the acceleration of gravity constant. The pressure drop is independent from the variation in the superficial velocity. It stays constant in the fluidization region, which goes from the minimum fluidization to the terminal velocity.

Minimum Fluidization Velocity

The transition point between fixed and fluidized bed is known as minimum fluidization velocity. It characterizes the minimum condition to initiate the fluidization, as expressed in

$$\frac{\Delta p}{H_{mf}} = (1-\epsilon_{mf})(\rho_p - \rho_g)g \ . \tag{2.30}$$

Figure 2.12 shows that at the point of minimum fluidization the pressure drop in the fluidized bed is equal to the pressure drop in the fixed bed. The pressure drop in the fixed bed can be calculated according to Ergun for minimum fluidization conditions as [7]

$$\frac{\Delta p_{mf}}{H_{mf}} = 150\frac{(1-\epsilon_{mf})^2}{{\epsilon_{mf}}^3}\frac{\mu U_{mf}}{(\phi d_P)^2} + 1.75\frac{1-\epsilon_{mf}}{{\epsilon_{mf}}^3}\frac{\rho_g {U_{mf}}^2}{\phi d_P} \ , \tag{2.31}$$

where μ is the viscosity of the gas, Δp_{mf} is the pressure drop in the fixed bed at the minimum fluidization point, and U_{mf} is the superficial velocity at the minimum fluidization point. Since at the minimum fluidization point $\Delta p_{fixed} = \Delta p_{fluid}$, the superficial velocity at minimum fluidization conditions, U_{mf}, can be found by combining (2.30) and (2.31)

$$(1-\epsilon_{mf})(\rho_p - \rho_g)g = 150\frac{(1-\epsilon_{mf})^2}{{\epsilon_{mf}}^3}\frac{\mu U_{mf}}{(\phi d_P)^2} + 1.75\frac{1-\epsilon_{mf}}{{\epsilon_{mf}}^3}\frac{\rho_g {U_{mf}}^2}{\phi d_P} \ . \tag{2.32}$$

Rearranging (2.32),

$$\frac{\rho_g(\phi d_P)^3(\rho_p - \rho_g)g}{\mu^2} = \frac{150(1-\epsilon_{mf})}{{\epsilon_{mf}}^3}\frac{\rho_g(\phi d_P)U_{mf}}{\mu} + \frac{1.75}{{\epsilon_{mf}}^3}\frac{\rho_g^2(\phi d_P)^2 {U_{mf}}^2}{\mu^2} \ , \tag{2.33}$$

or

$$Ar = C_1 Re_{p,mf} + C_2 Re_{p,mf}^2 \ . \tag{2.34}$$

Since (2.33) has a quadratic form the calculation of the minimum fluidization velocity, using this equation is not simple. However, one can prove [7][26] that the constants C1 and C2 stay nearly constant for different kinds of particles for a Reynolds number (Re_p) going from 0.001 until 4000. In such conditions, for fine particles, the following equation is valid [26].

$$U_L = \frac{\mu}{\rho_g d_P}[\sqrt{33.7^2 + 0.0408Ar} - 33.7] \ , \tag{2.35}$$

where Ar is the Archimedes number and can be calculated as

$$Ar = \frac{\rho_g {d_P}^3(\rho_P - \rho_g)g}{\mu^2} \ . \tag{2.36}$$

Terminal Velocity

The upper boundary of the fluidization region is given by the terminal velocity of the particle. It is defined as the free-fall velocity of a particle through a fluid and can be derived from fluid mechanics as [7][8]

$$U_t = \left[\frac{4d_P(\rho_s - \rho_g)g}{3\rho_g C_D}\right]^{1/2} \tag{2.37}$$

where C_D is an experimentally determined drag coefficient and according to Haider and Levenspiel [27] can be calculated as

$$C_D = \frac{24}{Re_P}\left[1 + (8.1716e^{-4.655\phi})Re_P^{0.0964+0.5565\phi}\right] + \frac{73.69e^{-5.0748\phi}Re_P}{Re_P + 5.378e^{62122\phi}} \tag{2.38}$$

And for spherical particles ($\phi = 1$), (2.38) can be reduced to

$$C_D = \frac{24}{Re_P} + 3.3643Re_P^{0.3471} + \frac{0.4607Re_P}{Re_P + 2682.5} \tag{2.39}$$

There are other correlations proposed to determine the drag coefficient C_D, depending on the conditions the particle is in. These can be found in the book of Yang [25], where the alternative forms to calculate the drag coefficient and the applicable conditions are very thoroughly explained.

2.4 Overview of the Circulating Fluidized Bed Process

In this work the properties of the combustion process in a circulating fluidized bed (CFB) will be studied, and for that the characteristics of this process will be presented in this section.

A circulating fluidized bed operates in the region of particle entrainment, which means that the particles on the bed have superficial velocities greater than their terminal velocity, as was depicted in Figure 2.12. A successful operation of a CFB has to meet some specifications concerning its design. A typical configuration of a CFB has four requirements: a tall vessel, also called riser, where the solids bed will be placed and the air will flow through it; a way in for solids, mostly at the bottom, where the recirculated solids and also the make-up will be (re)introduced in the vessel; a fluid flowing upward, with sufficient velocity to entrain the particles on the top of the solids bed; and ultimately a way to capture these particles, which is mostly a cyclone, and

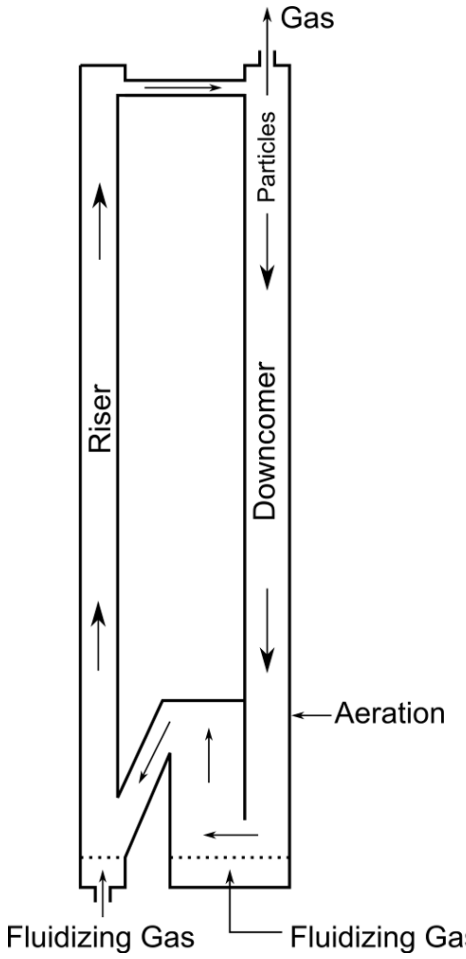

Figure 2.13: Typical configuration of a circulating fluidized bed [2]

to return it to the bottom of the vessel. Figure 2.13 depicts a typical set up for a CFB.

Comparing to other fluidized systems, the CFBs have a higher solid-gas contact, improving the mass/heat transfer rate between them. Also, the reduced axial gas dispersion in the vessel improves the homogeneity of the mixture. The addition of a recirculation step introduces a new variable in the system: the circulation flux, which grants a better control over the heat transferred from the suspension to the wall (isothermal operation). Furthermore, the solids loop gives the chance to execute a separate operation on the solids stream, which can be, for instance, recuperation, in case of a process which needs catalysts, or a heat transfer to utilize some of its heat. In spite of that, the recirculation also turns the system into something more complex, making the design and operation of such processes more difficult. The CFB requires a smaller cross-sectional area, due to its higher superficial velocity, which translates into a thinner vessel and, on the other hand, into an increased height. Apart from

a friction-resistant particle (for high velocities), the CFB has very little restrictions to the properties of particles being used, on account of the wide range of its allowed particle diameter (50μm<d_P <500μm), and of its lower susceptibility to particle aggregation and to the particle density.

2.5 Circulating Fluidized Bed Combustor

The CFB has been successfully employed in various applications, in particular in the Fluid Catalytic Cracking (FCC) [2], which is a well-known petroleum refining process, and in the Circulating Fluidized Bed Combustor (CFBC) [2], which is the process studied in this work.

A CFB applied to a combustion process brings advantages in comparison to other consolidated combustion technologies, specially to the combustion of biomass and other lower grade fuels [2]. For instance, the bed material in a CFBC is mostly composed of inert material (either sand, ash, or a sorbent) with the amount of solid fuel ranging from 0.5% to 5% of the total bed mass. The fuel is burned surrounded by those inert particles, and due to the high rates of heat and mass transfer the operation temperature is much lower than in other combustion technologies. Besides, the process can be operated at isothermal conditions which enables the burning of fuels with a high moisture content and reduces the pollutants emissions, particularly NO_x, which is the main concern on the combustion of solid fuels for power generation. The CFBC gives also the possibility to capture sulphur using a low-cost sorbent, typically limestone or dolomite, which hinders the necessity of the addition of scrubbers to the overall process, reducing the investment as well as the operation costs. Another noteworthy advantage of the CFB is its high turndown ratios (3:1 and more). Table 2.2 shows typical operation values of different combustion techniques.

	Bubbling bed	Circulating bed	Pulverized	Stoker fired
Gas Velocity [m/s]	1.5-3	4-8.5	4-6	1.2
Bed pressure drop [in H_2O]	80-100	40-70	-	-
Mean bed particle size [μ]	500-1500	150-500	-	-
Bed-surface heat transfer coefficient [W/m^{2}s]	300	120	-	-
Entrainment rate [kg/m^{2}s]	0.1-1	10-40	-	-
Excess air [%]	20-25	10-20	15-30	20-30
NO_x emission [ppmv]	100-300	50-200	400-600	400-600
Combustion efficiency [%]	90-96	85-99	99	85-90

Table 2.2: Operational points of some combustion systems for comparison [2].

The operating pressure on the CFBC may vary depending on the application. For instance, under atmospheric pressure the CFBC is used for steam generation and under high pressure, for combined-cycle applications. The operation temperature for the CFBC process ranges from 750°C to 950°C; bellow the lower limit, the rates of combustion are slow and the formation of CO and hydrocarbons due to an incomplete combustion may become a problem with the emissions. Also, the increase in temperature leads to the production of more NO_x, intensifying the pollution problem. Another problem that may come from increasing the operating temperature is the sintering of ash particles, forming agglomerates which block the bed fluidization and hinders the combustion. For CFBCs using more conventional combustion fuels, such as coal, it doesn't represent a major issue, since the high velocities of the bed tend to impede the formation of agglomerates. On the other hand, it can be an issue for fuels such as biomass due to its higher amount of alkali metals present in composition. When this problem is of significance, bed materials specially designed for avoiding agglomeration in the bed can be used. Another problem that the firing of biomass may bring is corrosion problems due to chlorine in its composition. A high content of chlorine in the fuel(0.1%) increases the hot corrosion potential, which is especially a concern for boilers operating at high steam temperature and pressure [28].

2.5.1 State of the Art

Due to its advantages, the CFB boiler is a promising technique for large scale energy production from biomass fuels [2][29][30]. In fact, it has shown some positive results in operating plants throughout the world. The current highest capacity for a CFB in operation with a pure biomass firing technology, namely the Advanced Biomass CFB, is of 205MW_e in the Polaniec power plant in Poland, with a fuel mixture of 80% wood residues and 20% agricultural residues [31], and the available technology scales up to 600 MW_e [32].

Another technique that has been used to increase the sustainability of the CFBC process is the OxyFuel. It uses a mixture of recycled flue gas and pure oxygen as the combustion air, resulting in a CO_2-rich flue gas which, without the addition of N_2 to hinder it, is very well suited for capture and storage. Better understanding of this technique can be found in the literature [33][10][34][35].

3 Modelling and Simulation

3.1 The Software IPSEpro

There are several ways to approach this particular problem and there exist many software applications to model it [2]. The choice of the best approach lies on the characteristics of the problem itself. The software program adopted here was the IPSEpro which is a simulation environment created primarily for applications in power plant technology. However, due to its flexible programming environment it can be applied to other process engineering areas, such as Flue Gas Cleaning, Thermal Power, Geothermal Energy, Concentrating Solar Power, Desalination, and Refrigeration [36]. It provides the prospect of modelling a process in an environment with a graphical flowsheet editor by connecting the model components through streams and then solving it mathematically. The characteristics of the models of the components and streams are comprised in a library, specific for each application. An example of a commercially available library is the APP_lib designed for power plant applications and the PGP_lib designed for pyrolysis and gasification processes [36].

IPSEpro comprises different modules each with different applications. The PSE (Process Simulation Environment) acts as the user interface where the flowsheet is built and the results of the simulations are displayed. The MDK (Model Development Kit) allows the user to change the standard models and also to create its own models accordingly. Additionally, there are the PSExcel and the PSEconomy models which, respectively, enables the use of MS Excel in connection with IPSEpro and the analysis and treatment the data obtained. Figure 3.1 shows how the software IPSEpro is structured.

The software IPSEpro adopts the equation-oriented solution strategy, meaning that all equations comprised in the models are solved simultaneously. Hence, the models are granted more flexibility regarding input and output of variables, the calculations are faster with less convergence problems, and it also enables dynamic calculations. However, the localization of errors is troublesome and providing a good initial guess is necessary. A way around this is by using an additional feature also implemented in the solver: the Lagrange multipliers method, which is an optimization method where the solution is the minimum of the sum of the squared residuals, as expressed by [37]

$$\sum_i \left(\frac{x_i - \bar{x}_i}{tol_{x_i}} \right)^2 \rightarrow min \ , \tag{3.1}$$

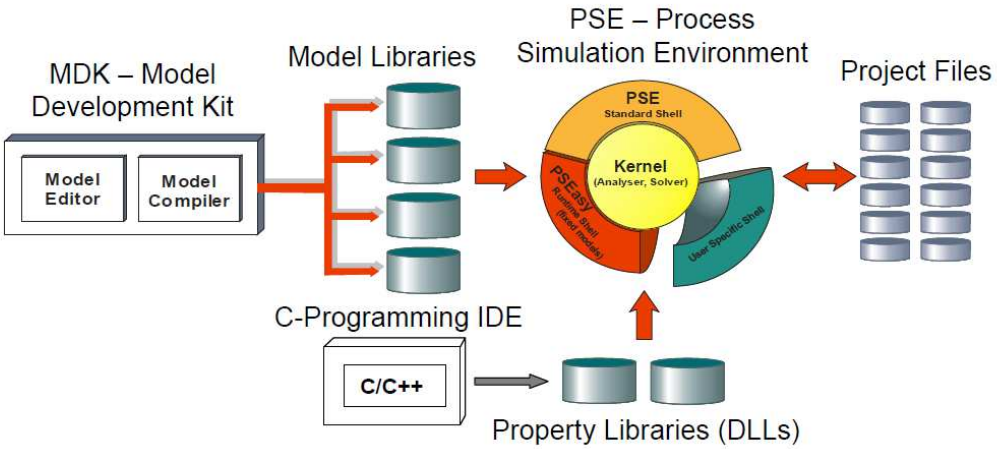

Figure 3.1: Structure of the software IPSEpro

where x_i is the measured value, $\bar{x}_i$ is the value predicted by the model, and tol_{x_i} is the absolute tolerance for x_i. The absolute tolerances establish the quality for each measure value. The localization of systematic errors, both in the simulation and measurements area, is achieved by comparing the resulting calculation errors and the estimated tolerance. Iteratively, by eliminating the found errors and adjusting the tolerances, the simulation results replicate the real process operation as accurately as allowed by the model limitations [37].

Concerning the CFBC process, IPSEpro brings an additional advantage, comparing to its standard modelling up until now, which is the possibility of a reliable representation of the solids flow, enabling the modelling of the recirculation sector.

3.2 Modelling

The mathematical modelling of a CFB combustor using biomass as fuel is very advantageous on its design and operation, since it promotes the better understanding of the process, predicting eventual problems that may arise during operation while avoiding costs with experimental set-ups. The ability to predict the behaviour regarding the combustion efficiency, clogging problems, and pollutants emissions, as well as the performance of different fuel types and mixture is very valuable for commercial applications.

3.2.1 Model Development

Some key steps must be followed when building a mathematical model. First, the system boundaries must be defined, then the parameters and variables of the system

must be determined, which are then correlated, forming the model equations.

The model equations should describe the particularities of the process as well as the physical phenomena occurring in its scope. The sections bellow discuss the group of model equations applied in the modelling of the CFB unit developed in this work.

Conservation of mass and energy

The conservation principle is considered through the whole model in steady state conditions. The mass balance was formulated differently depending on the conversion type that occurs inside the unit model. For instance, if there is a reaction taking place, a balance of the elements is calculated; if there are no chemical reactions, but the stream changes its composition (by either mixing or splitting), then a balance of the chemical compounds is then applied; and when the composition of the stream remains unchanged then a total mass flow balance is then of relevance. In the model the balance of elements was calculated for the elements C, H, O, N, S, Cl, and the general equation can be expressed as

$$\sum_{i=1}^{N} \dot{m}_{i,in} \cdot \frac{x_i w_{i,in}}{M_i} = \sum_{i=1}^{N} \dot{m}_{i,out} \cdot \frac{x_i w_{i,out}}{M_i} \tag{3.2}$$

where $\dot{m}$ is the mass flow rate, x_i is the molecular quantity of element i in the component, w_i is the mass fraction of the component which contains the element i, and M_i is atomic weight of the element i.

Inorganic substances are treated as chemically invariants and an species balance is then calculated as

$$\sum_{j=1}^{N} \dot{m}_{j,in} \cdot w_{j,in} = \sum_{j=1}^{N} \dot{m}_{j,out} \cdot w_{j,out} \tag{3.3}$$

Concerning the energy balances, the total enthalpy is the main contributor, while the kinetic and the potential energies are not considered. The energy balance can be written as

$$\dot{Q} + P = \sum_{i=1}^{N} \dot{n}_i \cdot H_i^*(p_i, T_i) \ , \tag{3.4}$$

where $\dot{Q}$, P, $\dot{n}_i$, $H_i^*(p_i, T_i)$ the net heat, the net mechanical power, the molar flow rate, and the total enthalpy, respectively. The molar flow rate changes signal depending on whether the stream is incoming (negative) or exiting (positive) the unit. The total enthalpy is defined as

$$H^*(p,T) = \Delta H^0_{f,298} + [H(p,T) - H(p_0,T_0)] \ , \tag{3.5}$$

where $\Delta H^0_{f,298}$ is the enthalpy of formation at standard conditions (p_0 = 1 bar, T_0 = 298,15 K).

Chemically bound energy

For comparison and practical purposes the energy of a fuel can be expressed in terms of the lower heating value (LHV). The fuel power is then expressed as

$$P_{th} = \dot{m} \cdot LHV \ , \tag{3.6}$$

where P_{th} is the thermal power of the fuel.

Chemical Reactions Model

No chemical equilibrium calculations where implemented in this model due to the assumption of complete combustion in the CFB unit. The incompleteness of the combustion reaction, even with a surplus of O_2, is expressed in terms of the ratio of CO/CO_2 in the exhaust gas, also called CO/CO_2 slip, and it is formulated as

$$CO_{slip} = \begin{cases} \frac{y_{CO,exh}}{y_{CO_2,exh}} \cdot 100 & \text{if } \lambda \geq 1 \\ \frac{2 \cdot y_{O_2,exh}}{y_{CO_2,exh}} \cdot 100 & \text{if } \lambda < 1 \end{cases} \tag{3.7}$$

where $y_{i,exh}$ is the composition in the exhaust gas. The amount and composition of organic char eventually contained in the ash drain must be specified regarding the case of incomplete fuel conversion.

The excess air ratio, λ, is defined for incomplete combustion as

$$\begin{aligned} &\lambda \left(\dot{m}_{exh} \left(w_{O_2,exh} - MM_{O_2} \cdot \sum_i \xi_i \frac{w_{i,exh}}{MM_i} + \right. \right. \\ &\left. \left. \dot{m}_{bed,out} \cdot \left[A_{bed,out} \left(w_{O,bed,out} - MM_{O_2} \cdot \sum_j \xi_j \frac{w_{j,bed,out}}{MM_i} \right) \right]_{char} \right) \right) \\ &= (1-\lambda) \dot{m}_{fluid} \cdot w_{O_2,fluid} \end{aligned} \tag{3.8}$$

where the index i represents the compounds that participate in the combustion reaction, the index j refers to the elements present in the char going out of the fluidized bed, $A_{bed,out}$ is the percentage amount of char in the solids stream out of the bed, and ξ_i is the stoichiometric index in the complete combustion reaction. In this set up the right side of the equation represents the total O_2 coming into the system and the left hand side presents the quantity of O_2 that would be present in the exhaust gas should the unconverted components be completely oxidized, including the potential of the solid carbon present in the ash to be fully oxidized.

Fluidization model

The modelling of the fludization in the combustion chamber is represented in terms of the superficial gas velocity at the riser exit, expressed as

$$U_{riser,exh} = \frac{\dot{V}_{riser,exh}}{A_{riser}} \ , \tag{3.9}$$

where A_{riser} is the cross-sectional area of the riser,$\dot{V}_{riser,exh}$ is the volume flow at the exit of the riser, and the specific solid transport rate, defined as

$$G_S = \frac{\dot{m}_{bed,out}}{A_{riser}}. \tag{3.10}$$

3.3 Implementation

3.3.1 Formulation of the CFB Unit

The first step was to design a CFB unit using the model equations described in the previous section. The CFB model represented in Figure 3.2 was developed to solve the energy and mass balances for a CFB combustor operating at oxidative conditions ($\lambda > 1$) and was then implemented in the IPSEpro environment. This first simulation was set up to emulate a typical CFB process as was previously depicted on Figure 1.2. The rest of the system was represented by standard units pre-existing in the model library PGP_lib. The cyclone is represented by the gas/solids separator unit and the cooling coil by a heat exchanger.

A couple of simulations were performed to check the consistency of the developed model with what is expected in the literature. The utilized fuel was spruce wood, a typical biomass fuel used for combustion purposes. Its composition is shown in Table 3.1 bellow.

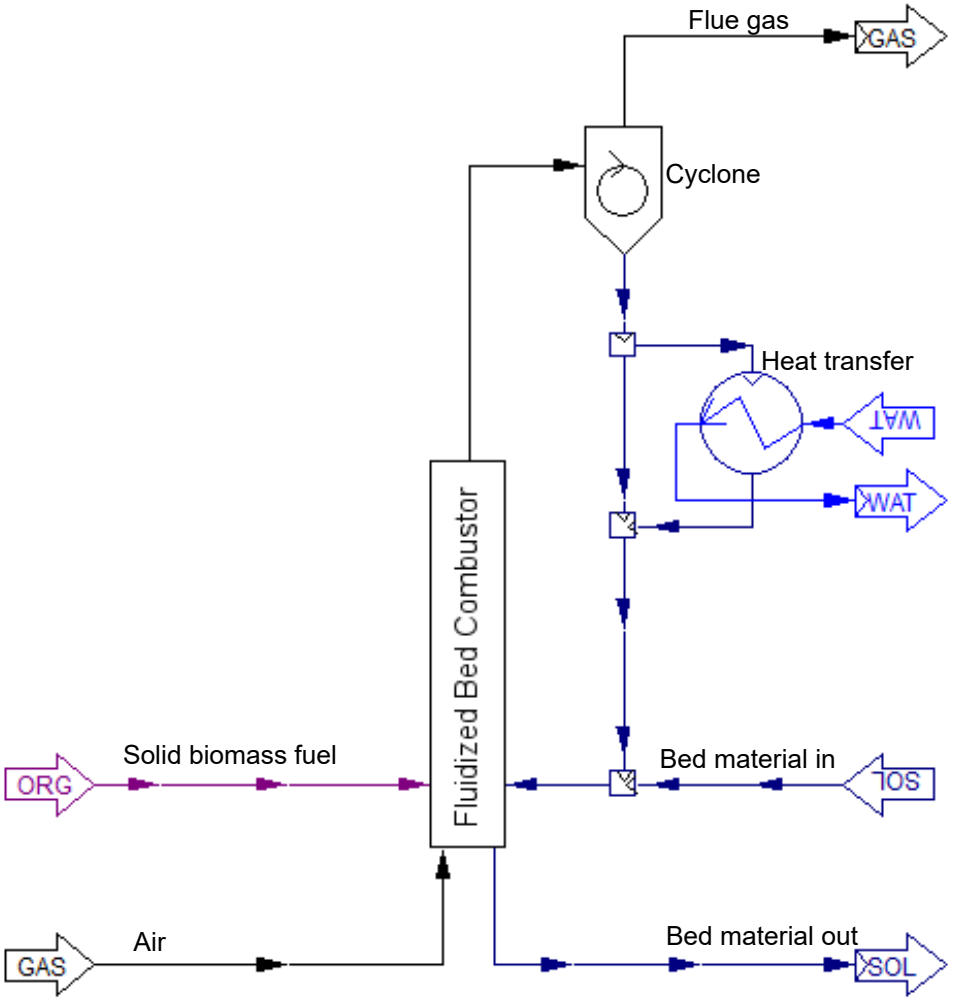

Figure 3.2: Flowsheet of the circulating fluidized bed combustion process in IPSEpro

3.3.2 Validation of the CFB Model Unit

Subsequently, the model previously developed was validated taking as basis the results presented by Wöß in his work [10]. The pilot plant described in his work was constructed in Gumpoldskirchen in a cooperation between Messer Austria GmbH and the Austrian Research Promotion Agency (FFG), and realized by Höltl during his PHD thesis [33]. The flowsheet illustrating the process taking place in the pilot plant, was built using the new CFB unit and other equipments already present on the PGPlib library, and it is depicted on Figure 3.3.

The pilot plant was designed for a thermal power of 100kW$_{th}$ which corresponds to a typical size of a pilot plant. The core of the system is a riser with a diameter of 0.15m and a height of 5m, and it is possible to introduce the fluidizing gas at two

Fuel Composition	
	Spruce Wood with Bark
Water [w%]	15
Ash [w%] (wf)	0.6
C [w%] (waf)	49.8
H [w%] (waf)	6.3
O [w%] (waf)	43.15
N [w%] (waf)	0.13
S [w%] (waf)	0.015
Cl [w%] (waf)	0.005

Table 3.1: Elementary composition of the fuel used for the simulation of the CFBC model

different locations (primary and secondary fluidization). In this type of reactor, the bed material (quartz sand) is fluidized by a mixture of a flue gas and pure oxygen at the reactor bottom. Therefore a good gas-solid mixture is to be ensured, thus enabling homogeneous distribution of the fuel within the reactor.

After the reactor, the gas-solid mixture is separated in a cyclone, which allows a high degree of gas-solids separation. After deposition, the particles get into a siphon, which can be fluidized with pure CO_2 or air. It is possible to cool the recirculated solids in a cooling coil before it goes back into the reactor. The cooling capacity can be adjusted by the screw speed and the cooling of the screw occurs with cooling water. The fraction that doesn't passes through the coil circulates back into the reactor bed uncooled.

In order to guarantee the necessary residence time in the reactor system, after the cyclone the gas passes into a post-combustion chamber. This allows a "polishing" of the exhaust gas in the case of incomplete combustion, ensuring a as complete as possible overall combustion of the fuel. The exhaust gas is cooled subsequently through a variable heat exchanger, depending on the dew point of the gas, down to about 170°C to 220°C. This temperature range allows to posteriorly segregate the exhaust particulate matter, which is done in a bag filter designed for a maximum flue gas inlet temperature of 250°C. The cooled and particulate-matter-free exhaust gas passes through a chimney to the outside or it can be recycled back into the system via a compressor [33][10][34].

In the experiments conducted by Wöß two types of fuel were tested: industrial and municipal sewage sludge. However, on behalf of simplicity, on the simulations performed in this work, only one type of fuel was set in the simulation environment, since both fuels present a similar composition with slight variations in the calorific value [10].

The fuel chosen to run the validation of the model in this work was a type of sewage sludge which was analysed by Wöß. As a result of this analysis the elemental com-

position, as well as the water and ash content could be determined. The resulting composition is presented in Table 3.2. As a result of the same analysis, it is reported that the composition of some heavy metals exceeded the limit specified for use in agricultural applications and/or for composting, which makes the experimented fuel a good candidate for burning applications.

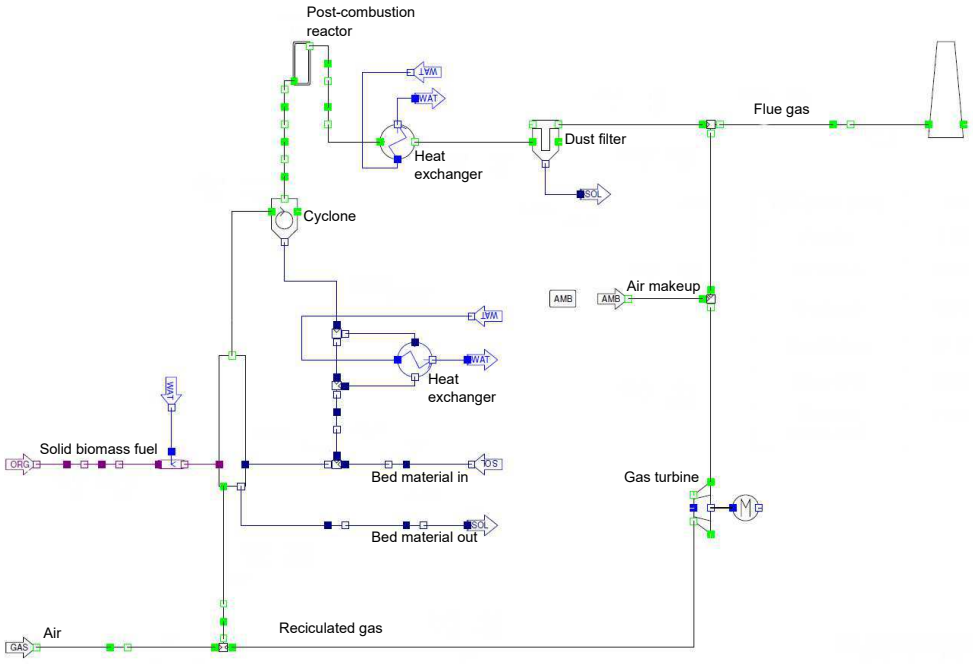

Figure 3.3: Flowsheet of the CFBC pilot plant in IPSEpro

Sewage Sludge Composition	
Water [w%]	10.28
Ash [w%] (wf)	31.29
C [w%] (waf)	53.16
H [w%] (waf)	5.26
O [w%] (waf)	34.10
N [w%] (waf)	6.25
S [w%] (waf)	1.23
Cl [w%] (waf)	0.00

∗waf = water and ash free

∗wf = water free

Table 3.2: Elementar composition of the sewage sludge used as fuel [10]

3.3.3 Application of the Model Unit in the Co-combustion of biomass and waste

After having the model validated by a concrete example, the next step was to apply the model to a simulation using a combination of biomass and waste as fuel for the CFBC model.

Co-combustion of biomass with other fuels is a simple and economically suitable way to replace fossil fuels in existing power plants by biomass and to re-purpose waste. However, the combination of different kinds of fuels can cause positive or negative synergy effects. One of these effects is the interaction between some components present in the fuels (alkali metals, for instance) which can lead to the formation of deposits inside the boiler or to contribute to the formation of dioxins[9]. Understanding how those interactions work can be of great advantage as it can help to promote the positive effects and to avoid the negative ones. Figure 3.4 shows the main synergy effects which occur during the process of co-combustion, according to the elements present in the fuel composition.

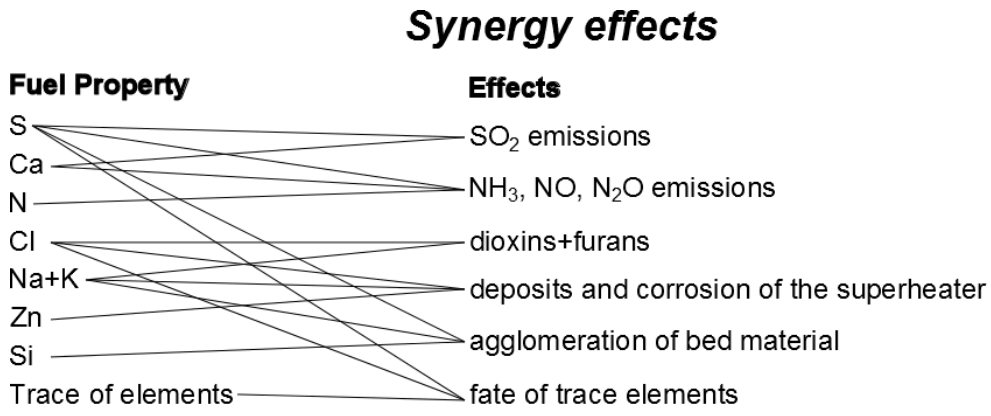

Figure 3.4: Synergy effects between fuels in co-combustion processes [9]

As seen in the previous sections of this chapter, the advantages a CFBC brings, makes it a fitting process for a variety of fuel qualities and moistures, for example wood and other biomass types. A range of technologies could be applied for the co-firing process, however, the use low grade fuels is the most attractive feature of this process, and in this case the CFBC may be the most suitable technology for this application.

The simulation of the co-firing process of biomass and waste was carried out using the same process flowsheet depicted in Figure 3.5. The fuels used were a combination of sewage sludge and spruce with the same composition as shown in Tables 3.1 and 3.2. The operational parameters were set differently to better fit the process and are shown on Table 3.3.

The simulations described in this chapter were divided into three parts: Simple CFBC Simulation (Section 3.3.1), Simulation of the Pilot Plant (Section 3.3.2), and Simula-

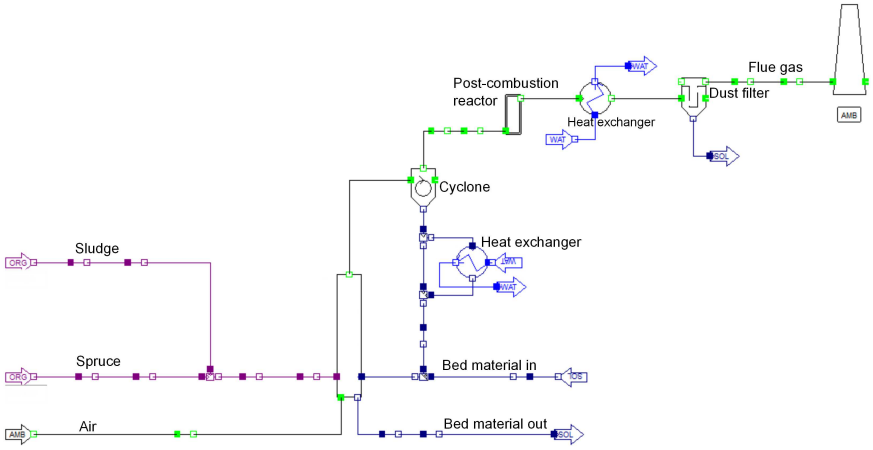

Figure 3.5: Flowsheet of the co-combustion process

Combustor	
Thermal Capacity (kW_{th})	40.0
Pressure drop on CFB (bar)	0.2
Excess air ratio(λ)	1.5
Fluidization velocity (m/s)	4.0

Table 3.3: Operational parameters for the simulation of the co-firing process

tion of the Co-combustion of Wood and Sewage Sludge (Section 3.3.3). The results will be displayed and discussed along the next sections of this chapter.

4 Results and Discussion

This chapter presents the evaluation procedure for the CFB model developed previously. First, a series of simulations were performed varying some key parameters in order to verify the sensitivity of the model in respect to a particular set of variables. Second, the model was tested on its capability to predict the experimental results of an existent plant, using the data observed by Wöß. Ultimately, a simulation of a co-combustion process was carried out.

4.1 Simple CFBC Simulation

In this section, the model performance is tested by varying selected parameters and comparing its effects on selected outputs using a design of experiments approach. This technique enables the determination of individual and interactive effects of the inputs that could affect the output, assuming that the variables are independent.

There are three aspects of the process analysed by a designed experiment. Factors are inputs to the process and can be classified as either controllable or uncontrollable variables; the levels are the settings of each factor in the study; and the response or outputs of the experiment, which are measurable outcomes potentially influenced by the factors and their respective levels.

Designed experiments have many potential uses in improving processes, such as comparing alternatives, identifying the significant inputs affecting an output, achieving an optimal process output, reducing variability, and improving process robustness.

For the sake of simplicity of this evaluation, four parameters were chosen as factors: temperature of the solids bed, fuel moisture, excess air ratio, and superficial velocity at the riser exit; and each factor was assigned three levels, which means the values the factors should assume in the simulations. The investigated outputs were the thermal energy in the reactor,and the O_2 and NO output concentrations. This is summarized in Table 4.1.

The simulations were carried out in order to evaluate the paired influences of the factors, meaning that the currently evaluated factors were set to its maximum and minimum values while the others were conserved in their medium values, to determine whether the chosen inputs were significantly affecting the observed outputs. Table 4.2 outlines how the experiments were executed.

Input Values				
		-1(min)	0(medium)	1(max)
Lambda [-]	X1	0.9	1.65	2.4
Moisture [%]	X2	5	30	55
BedT [°C]	X3	600	825	1050
SupVel [m/s]	X4	5	10	15
Outputs				
Y1		Gas Composition out		O_2 conc
Y2		Enegy		P_therm
Y3		Gas Composition out		NO conc

Table 4.1: Input factors and output variables chosen for the simulations

4.1.1 Results

The 24 simulations were carried out and the results are summarized in Table 4.3 below. In Table 4.3 the symbol "+" refers to the average result of the outputs of the particular set of experiments where the respective factor is at its maximum value, the symbol "-" to the average result of the outputs of the particular set of experiments where the respective factor is at its minimum value and the slope is the intensity of the variation between these two points. One can define the impact of the an input in a specific output by analysing the absolute value of the slope.

From the results in Table 4.3, it is possible to determine the factor with the most influence on the chosen outputs, as shown in Table 4.4 and on the diagramms in Figure 4.1. For instance, the output O_2 concentration (Y1) is most influenced by the excess air ratio (X1) followed by the moisture (X2). This is also true for the NO concentration (Y3). The energy in the reactor, on the other hand, is impacted by 3 factors (X1,X3, and X4), not making it possible to determine which one has the most influence within this set of experiments. Therefore, in this particular case the three inputs should be accounted and should not be neglected, if the energy in the reactor is a sensitive output for the analysis. This might suggest that these parameters may also have an impact on each other, thus the assumption of independence of variables may not be valid for this case. For this output, it can be asserted that, among the set of tried factors, the moisture (X2) has the least influence regarding the energy in the reactor.

Exp	Sim#	X1	X2	X3	X4
1	1	1	1	0	0
	2	-1	1	0	0
	3	1	-1	0	0
	4	-1	-1	0	0
2	5	1	0	1	0
	6	-1	0	1	0
	7	1	0	-1	0
	8	-1	0	-1	0
3	9	1	0	0	1
	10	-1	0	0	1
	11	1	0	0	-1
	12	-1	0	0	-1
4	13	0	1	1	0
	14	0	-1	1	0
	15	0	1	-1	0
	16	0	-1	-1	0
5	17	0	1	0	1
	18	0	-1	0	1
	19	0	1	0	-1
	20	0	-1	0	-1
6	21	0	0	1	1
	22	0	0	-1	1
	23	0	0	1	-1
	24	0	0	-1	-1

Table 4.2: Design of experiments

		Main effects											
		X1			X2			X3			X4		
Exp		Y1	Y2	Y3	Y1	Y2	Y3	Y1	Y2	Y3	Y1	Y2	Y3
1	+	11.015	30.829	0.0167	5.277	42.522	0.0248						
	-	0.0654	69.609	0.0376	5.803	57.916	0.0295						
	Slope	5.475	-19.390	-0.0104	-0.2634	-7.697	-0.0024						
2	+	11.098	33.832	0.0168				5.582	43.488	0.0274			
	-	0.0661	73.942	0.0380				5.582	64.286	0.0274			
	Slope	5.516	-20.055	-0.0106				0.000	-10.399	0.0000			
3	+	11.098	31.392	0.0168							5.582	76.672	0.0274
	-	0.0661	70.838	0.0380							5.582	25.557	0.0274
	Slope	5.516	-19.723	-0.0106							0.000	25.557	0.0000
4	+				6.481	37.741	0.0211	7.042	35.885	0.0229			
	-				7.603	50.723	0.0248	7.042	52.579	0.0229			
	Slope				-0.561	-6.491	-0.0018	0.000	-8.347	0.0000			
5	+				6.481	35.018	0.0211				7.042	62.709	0.0229
	-				7.603	48.593	0.0248				7.042	20.903	0.0229
	Slope				-0.561	-6.787	-0.0018				0.0000	20.903	0.0000
6	+							7.202	36.306	0.0234	7.202	68.491	0.0234
	-							7.202	55.016	0.0234	7.202	50.339	0.0234
	Slope							0.000	-9.355	0.000	0.000	9.076	0.000

Table 4.3: Results of the design of experiments simulations

Exp	Y1	Y2	Y3
1	*X1*	*X1*	*X1*
2	*X1*	*X1*	*X1*
3	*X1*	*X4*	*X1*
4	*X2*	*X3*	*X2*
5	*X2*	*X4*	*X2*
6	*X3/X4*	*X3*	*X3/X4*

Table 4.4: Factors with the most effect per experiment

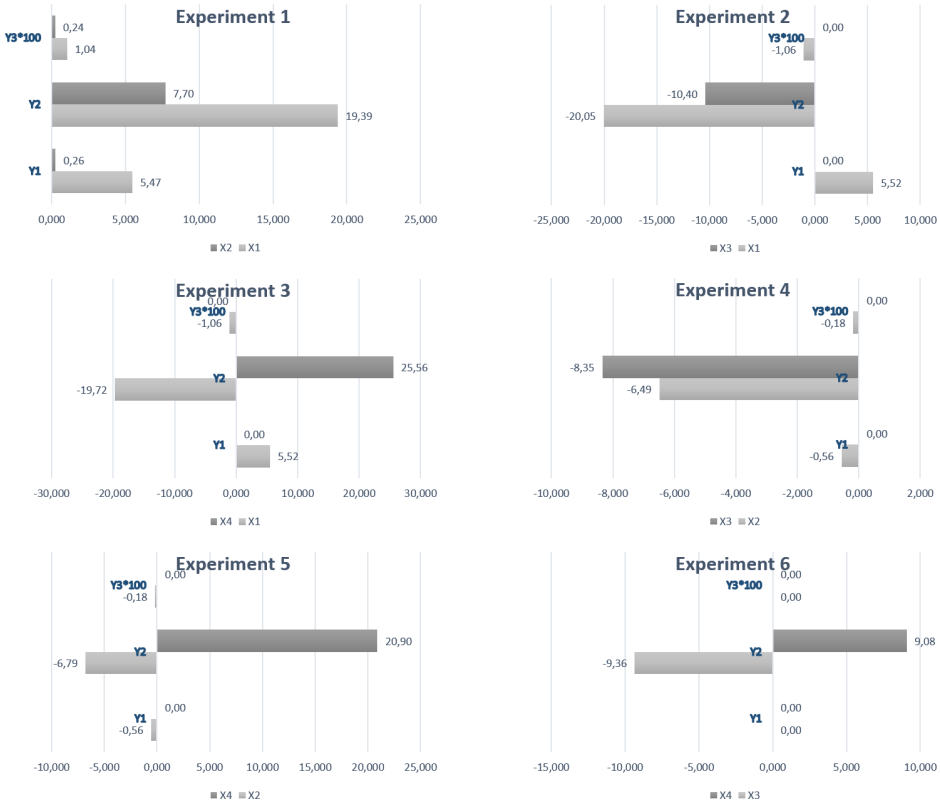

Figure 4.1: Effect of factors on the selected outputs per experiment

4.2 Simulation of the Pilot Plant

In this section, the model efficiency is proved on its ability to predict a concrete experimental set up, namely the pilot plant described in the previous chapter. The

experiments were conducted in six different operational points defined in the diagram depicted by Figure 4.2.

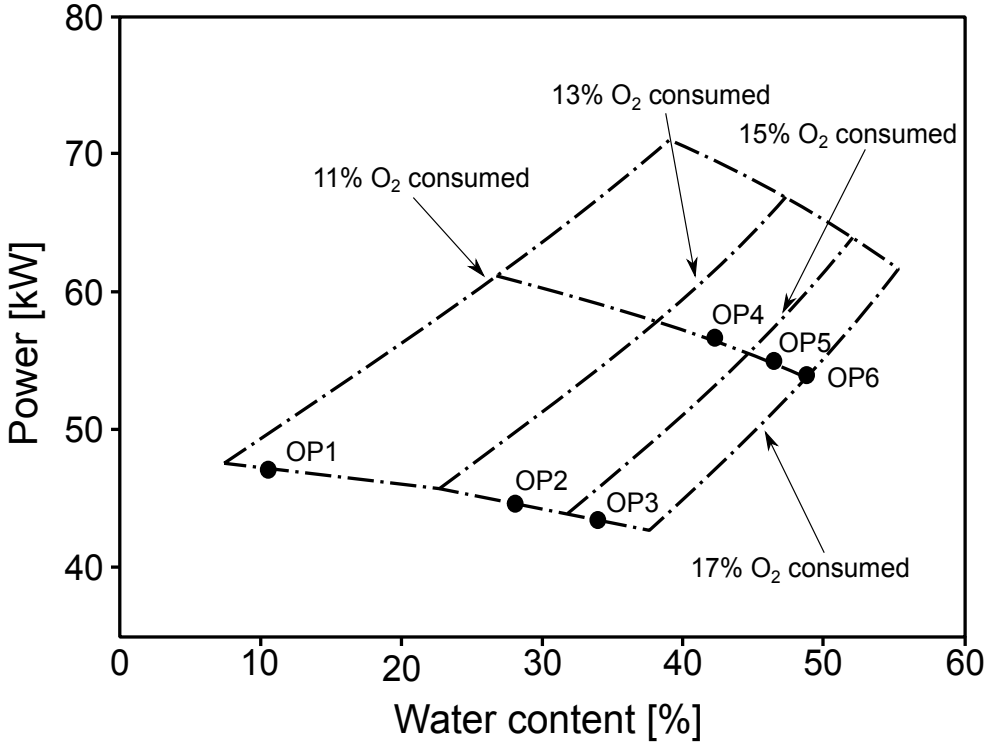

Figure 4.2: Operational points considered for the simulation of the pilot plant [10]

The input values for every operation point is shown in Table 4.5 bellow.

Using the values on Table 4.5 as inputs, each point was simulated separately and the results are shown in Tables 4.6 and 4.7. The simulation results are quite similar within a margin, thus validating the model developed in the previous chapter.

		OP1	*OP1_P*	*OP2*	*OP3*	*OP4*	*OP5*	*OP6*
				Riser				
dp_{gas}	[mbar]	10,00	10,00	10,00	10,00	10,00	10,00	10,00
Lambda	[-]	1,79	1,77	1,98	1,75	1,52	1,55	1,69
Cross-sectional area [%]	[m^2]	0,01	0,01	0,01	0,01	0,01	0,01	0,01
Superficial velocity	[m/s]	7,08	6,98	7,06	6,39	9,40	8,88	9,05
Bed Temperature	[°C]	879,00	879,00	879,00	879,00	879,00	886,00	879,00
Power	[kW]	47,12	47,12	44,68	42,37	56,74	55,04	54,02
				Wet Fuel				
Pressure	[bara]	1,20	1,20	1,10	1,10	1,10	1,10	1,10
Temperature	[°C]	20,00	20,00	17,79	16,96	16,80	16,57	16,46
Water content	[%]	10,58	10,58	28,13	39,43	42,28	46,58	48,87
Ash content	[%]	31,29	31,29	25,15	21,19	20,20	18,69	17,89
				Fluidization Gas				
Temperature	[°C]	44,47	44,65	56,99	61,77	45,12	55,06	61,62
O_2 concentration	[vol%]	20,95	20,76	24,35	25,80	20,70	23,84	25,79
O_2 concentration in flue gas	[%]	8,42	8,29	10,45	8,82	5,62	6,35	7,82

Table 4.5: Input values applied to the operational points of the pilot plant simulation

		Simulation Results		Woss results	
		Fluidization gas	Flue gas	Fluidization gas	Flue gas
OP1	p [bara]	***1.15***	***1.00***	1.15	1.00
	T [C]	***45.31***	***136.97***	44.48	136.97
	Nvol flow [Nm3/h]	***76.98***	***83.89***	69.29	85.02
	Massflow [kg/h]	***98.88***	***108.98***	89.07	110.50
	O2 conc [vol%]	***20.95***	***8.02***	20.95	8.42
	O2 infeed [Nm3/h]	***16.13***	***6.73***	14.52	7.16
	O2 consumed	-	*42%*	-	*49%*
OP1_P	p [bara]	***1.15***	***1.00***	1.15	1.00
	T [C]	***45.46***	***136.97***	44.65	136.97
	Nvol flow [Nm3/h]	***75.95***	***83.25***	68.08	83.82
	Massflow [kg/h]	***97.56***	***107.66***	87.46	108.95
	O2 conc [vol%]	***21.00***	***8.29***	21.00	8.29
	O2 infeed [Nm3/h]	***15.95***	***6.90***	14.30	6.95
	O2 consumed	-	*43%*	-	*49%*
OP2	p [bara]	***1.15***	***1.00***	1.15	1.00
	T [C]	***60.67***	***136.97***	58.48	136.97
	Nvol flow [Nm3/h]	***73.22***	***85.07***	64.60	84.78
	Massflow [kg/h]	***94.51***	***108.19***	83.51	108.53
	O2 conc [vol%]	***24.37***	***10.45***	25.14	10.45
	O2 infeed [Nm3/h]	***17.84***	***8.89***	16.24	8.86
	O2 consumed	-	*50%*	-	*55%*
OP3	p [bara]	***1.15***	***1.00***	1.15	1.00
	T [C]	***71.72***	***136.97***	64.55	136.97
	Nvol flow [Nm3/h]	***63.19***	***79.45***	52.34	76.77
	Massflow [kg/h]	***81.52***	***98.62***	67.84	96.27
	O2 conc [vol%]	***25.00***	***8.82***	26.96	8.82
	O2 infeed [Nm3/h]	***15.80***	***7.01***	14.11	6.77
	O2 consumed	-	*44%*	-	*48%*

Table 4.6: Results Comparison of the Power Plant Simulation

		Simulation Results		Woss results	
		Fluidization gas	Flue gas	Fluidization gas	Flue gas
OP4	p [bara]	***1.15***	***1.00***	1.15	1.00
	T [C]	***87.89***	***136.97***	44.65	136.98
	Nvol flow [Nm3/h]	***88.79***	***112.42***	81.00	112.91
	Massflow [kg/h]	***113.51***	***138.28***	104.13	140.22
	O2 conc [vol%]	***21.00***	***5.62***	21.00	5.62
	O2 infeed [Nm3/h]	***18.65***	***6.32***	17.01	6.35
	O2 consumed	-	*34%*	-	*37%*
OP5	p [bara]	***1.15***	***1.00***	1.15	1.00
	T [C]	***52.95***	***179.98***	56.37	179.98
	Nvol flow [Nm3/h]	***77.65***	***104.30***	70.92	105.94
	Massflow [kg/h]	***100.29***	***127.55***	91.62	130.20
	O2 conc [vol%]	***24.51***	***6.35***	24.51	6.35
	O2 infeed [Nm3/h]	***19.03***	***6.62***	17.38	6.73
	O2 consumed	-	*35%*	-	*39%*
OP6	p [bara]	***1.15***	***1.00***	1.15	1.00
	T [C]	***59.61***	***136.97***	63.68	130.98
	Nvol flow [Nm3/h]	***77.74***	***106.21***	71.81	108.70
	Massflow [kg/h]	***100.76***	***129.52***	93.04	133.13
	O2 conc [vol%]	***26.70***	***7.82***	26.70	7.82
	O2 infeed [Nm3/h]	***20.76***	***8.31***	19.17	8.50
	O2 consumed	-	*40%*	-	*44%*

Table 4.7: Continuation: Results Comparison of the Power Plant Simulation

4.3 Simulation of the Co-combustion of Wood and Sewage Sludge

The simulation of the effects of the co-combustion of a mixture of spruce and sewage sludge, described in Section 3.3.3 was carried out according to the process described by the flowsheet in Figure 3.5 and using the operational parameters given by Table 3.3. First, the thermal efficiency of the process is calculated according to

$$\eta_{th} = \frac{OutputEnergy}{InputEnergy}, \tag{4.1}$$

where the input is represented by the energy carried in by the input streams of fuel (spruce and sludge), bed material, and air, and the outputs by the gas and the solids drain. The results are shown in the Table 4.8 bellow.

Energy Input [MJ/h]	
Spruce	135.23
Sludge	22.27
Air	1.89
Solids bed	2.31
Energy Output [MJ/h]	
Gas drain	16.26
Solids drain	66.14
Thermal efficiency	50.96%

Table 4.8: Thermal efficiency of the co-combustion process

The thermal efficiency of 50.96% is a good value, specially for low grade fuels.

The simulation of the separate combustions of spruce and coal were also carried out to be used as a mean of comparison and to observe the deviations by mixing a lower grade fuel(sludge). The gas drain composition is shown on Table 4.9. The comparison with the values for the separate combustions of spruce and coal shows that the emissions values for the Co-combustion don't diverge much from the results of the spruce combustion, and are quite good comparing it with the results of coal combustion, demonstrating once again he advantage of the Co-combustion process.

Gas drain composition	
wAr [kg/kg]	0.0071
wC2H4[kg/kg]	0.0000
wC2H6 [kg/kg]	0.0000
wC3H8 [kg/kg]	0.0000
wCH4 [kg/kg]	0.0000
wCO [kg/kg]	0.0006
wCO2 [kg/kg]	0.1759
wH2 [kg/kg]	0.0000
wH2O [kg/kg]	0.0788
wH2S [kg/kg]	0.0000
wHCl [kg/kg]	0.0000
wHCN [kg/kg]	0.0000
wN2 [kg/kg]	0.6669
wN2O [kg/kg]	0.0000
wNH3 [kg/kg]	0.0000
wNO [kg/kg]	0.0017
wO2 [kg/kg]	0.0687
wSO2 [kg/kg]	0.0003

Table 4.9: Gas drain composition of the co-combustion of sludge and wood

Gas drain composition		
	Spruce	Coal
wAr [kg/kg]	0.0126	0.0130
wC2H4 [kg/kg]	0.0000	0.0000
wC2H6 [kg/kg]	0.0000	0.0000
wC3H8 [kg/kg]	0.0000	0.0000
wCH4 [kg/kg]	0.0000	0.0000
wCO [kg/kg]	0.0009	0.0011
wCO2 [kg/kg]	0.1368	0.1672
wH2 [kg/kg]	0.0000	0.0000
wH2O [kg/kg]	0.0560	0.0345
wH2S [kg/kg]	0.0000	0.0000
wHCl [kg/kg]	0.0000	0.0001
wHCN [kg/kg]	0.0000	0.0000
wN2 [kg/kg]	0.6874	0.7089
wN2O [kg/kg]	0.0000	0.0000
wNH3 [kg/kg]	0.0000	0.0000
wNO [kg/kg]	0.0002	0.0018
wO2 [kg/kg]	0.1061	0.0723
wSO2 [kg/kg]	0.0000	0.0012

Table 4.10: Gas drain results of the simulations of the combustions of Coal and Spruce

5 Conclusions and Outlook

This work offers simulation models that are appropriate for use for evaluating the circulated fluidized bed combustor effects.

As well known, simulations are of an assumptive nature and its results feasibility depends greatly on the amount and quality of the data in which the simulation is applied. One way to approach the assumptive nature of the simulation task is to recognize that reality conditions or constraints in the models need to be examined systematically across a range of plausible conditions. This implies that multiple analyses under systematically varied conditions that are based upon principles of parametric experimental design are needed.[38] This was the goal of the Simple CFBC Simulation using a design of experiments analysis approached in Section 4.1.

Furthermore, the system analysis can be simplified if a complete sensitivity analysis would be performed to the entire plant, as it was demonstrated here in Section 4.1 for a very limited set of inputs. There one can determine the degree of influence of each input in the system, choose the most important factors and, then it would be possible to work on a more simplified version - where only the most significant inputs would be presented - to obtain a better design.

This approach could also be applied for the co-combustion process in order to identify whether there are any major differences from the combustion of one fuel at a time, as well as to determine the parameters with the most influence on the operation of this process.

Bibliography

[1] Institute for Energy Research (IER). (2012, December) Fossil fuels still king in EIA's annual energy outlook 2013. IER. [Online]. Available: http://instituteforenergyresearch.org/analysis/fossil-fuels-still-king-in-eias-annual-energy-outlook-2013/

[2] J. R. Grace, A. A. Avidan, and T. M. Knowlton, *Circulating fluidized beds*. Blackie Academic & Professional Glasgow, UK, 1997.

[3] S. Van Loo and J. Koppejan, *The Handbook of Biomass Combustion and Co-firing*. Earthscan, 2008.

[4] V. F. Ferreira, D. R. d. Rocha, and F. d. C. d. Silva, "Potencialidades e oportunidades na química da sacarose e outros açúcares," *Química Nova*, vol. 32, pp. 623 – 638, 00 2009. [Online]. Available: http://www.scielo.br/scielo.php?script=sci_arttext&pid=S0100-40422009000300007&nrm=iso

[5] M. Kaltschmitt, H. Hartmann, and H. Hofbauer, *Energie aus Biomasse*. Springer, 2009.

[6] T. Nussbaumer, "Combustion and co-combustion of biomass: fundamentals, technologies, and primary measures for emission reduction," *Energy & fuels*, vol. 17, no. 6, pp. 1510–1521, 2003.

[7] D. Kunii and O. Levenspiel, *Fluidization Engineering*, 2nd ed. Butterworth-Heinemann, 1991.

[8] H. Hofbauer, "Unterlagen zur Vorlesung Wirbelschichttechnik (SS 2013)," 2013.

[9] B. Leckner, "Co-combustion: A summary of technology," *Thermal Science*, vol. 11, no. 4, pp. 5–40, 2007.

[10] D. Wöß, ""Sauerstoff statt Stützbrennstoff": Sauerstoffangereicherte Verbrennung von niedrigkalorischen Festbrennstoffen in einer zirkulierenden Wirbelschicht," Master's thesis, Technische Universität Wien, 2012.

[11] D. L. Klass, *Biomass for Renewable Energy, Fuels, and Chemicals*. Academic press, 1998.

[12] World Energy Council (WEC), "World energy resources: 2013 survey," World Energy Council, Tech. Rep., 2013. [Online]. Available: www.worldenergy.org

[13] M. E. Walsh, G. Daniel, H. Shapouri, and S. P. Slinsky, "Bioenergy crop production in the united states: potential quantities, land use changes, and economic impacts on the agricultural sector," *Environmental and Resource Economics*, vol. 24, no. 4, pp. 313–333, 2003.

[14] Energy research Centre of the Netherlands (ECN). ECN phyllis classification. [Online]. Available: https://www.ecn.nl/phyllis2/

[15] IEA Bioenergy Task 32. BioBank. [Online]. Available: http://www.ieabcc.nl/

[16] Technische Universität Wien. BIOBIB - a database for biofuels. [Online]. Available: http://www.vt.tuwien.ac.at/biobib/

[17] P. McKendry, "Energy production from biomass (part 1): overview of biomass," *Bioresource technology*, vol. 83, no. 1, pp. 37–46, 2002.

[18] B. Jenkins, L. Baxter, T. Miles Jr, and T. Miles, "Combustion properties of biomass," *Fuel processing technology*, vol. 54, no. 1, pp. 17–46, 1998.

[19] J. Hu, F. Yu, and Y. Lu, "Application of Fischer–Tropsch synthesis in biomass to liquid conversion," *Catalysts*, vol. 2, no. 2, pp. 303–326, 2012.

[20] A. Steynberg and M. Dry, *Fischer-Tropsch Technology*. Elsevier, 2004.

[21] D. A. Mitchell, M. Berovič, and N. Krieger, *Solid-state fermentation bioreactor fundamentals: introduction and overview*. Springer, 2006.

[22] A. Pandey and C. Larroche, *Biofuels: alternative feedstocks and conversion processes*. Academic Press, 2011.

[23] M. E. Himmel, J. O. Baker, R. P. Overend *et al.*, *Enzymatic conversion of biomass for fuels production*. American Chemical Society, 1994.

[24] R. G. Holdich, *Fundamentals of particle technology*. Midland Information Technology and Publishing, 2002.

[25] W.-c. Yang, *Handbook of fluidization and fluid-particle systems*. CRC Press, 2003.

[26] C. Wen and Y. Yu, "A generalized method for predicting the minimum fluidization velocity," *AIChE Journal*, vol. 12, no. 3, pp. 610–612, 1966.

[27] A. Haider and O. Levenspiel, "Drag coefficient and terminal velocity of spherical and nonspherical particles," *Powder technology*, vol. 58, no. 1, pp. 63–70, 1989.

[28] P. Basu, *Combustion and gasification in fluidized beds*. CRC press, 2006.

[29] R. Van den Broek, A. Faaij, and A. van Wijk, *Biomass combustion for power generation*. Elsevier, 1996, vol. 11, no. 4.

[30] K. Yamamoto, "Biomass power generation by CFB boiler," *NKK Technical Report*, pp. 22–26, 2001.

[31] Power Engineering International. (2013, November) Is CFB the key to scaling up biomass? [Online]. Available: http://www.powerengineeringint.com/articles/print/volume-21/issue-10/features/is-cfb-the-key-to-scaling-up-biomass.html

[32] power-technology.com. Polaniec biomass power plant, Poland. [Online]. Available: http://www.power-technology.com/projects/polaniec-biomass-power-plant-poland/

[33] W. Höltl, "OxyFuel-Verbrennung in einer zirkulierenden Wirbelschicht: Auslegung, Konstruktion und Inbetriebnahme einer 100 kWth Versuchsanlage," Ph.D. dissertation, Technische Universität Wien, 2010.

[34] G. Tondl, "OxyFuel Verbrennung von Klärschlamm," Ph.D. dissertation, Technische Universität Wien, 2013.

[35] W. Höltl, T. Pröll, J. Rohovec, B. Kronberger, and H. Hofbauer, "Oxyfuel combustion of alternative fuels in a circulating fluidized bed combustor-design of a 100 kW test unit," in *ECM 2009 FOURTH EUROPEAN COMBUSTION MEETING, 14 - 17 April 2009, Vienna University of Technology, Vienna, Austria*, 2009.

[36] Simtech. (2014) IPSEpro description. [Online]. Available: http://www.simtechnology.com/CMS/index.php/ipsepro

[37] J. Bolhàr-Nordenkampf, T. Pröll, P. Kolbitsch, and H. Hofbauer, "Comprehensive modeling tool for chemical looping based processes," *Chemical engineering & technology*, vol. 32, no. 3, pp. 410–417, 2009.

[38] W. M. Trochim. Computer simulations for research design. [Online]. Available: http://www.socialresearchmethods.net/simul/conclude.htm